Copyright Warning & Restrictions

The copyright law of the United States (Title 17, United States Code) governs the making of photocopies or other reproductions of copyrighted material.

Under certain conditions specified in the law, libraries and archives are authorized to furnish a photocopy or other reproduction. One of these specified conditions is that the photocopy or reproduction is not to be "used for any purpose other than private study, scholarship, or research." If a, user makes a request for, or later uses, a photocopy or reproduction for purposes in excess of "fair use" that user may be liable for copyright infringement,

This institution reserves the right to refuse to accept a copying order if, in its judgment, fulfillment of the order would involve violation of copyright law.

Please Note: The author retains the copyright while the New Jersey Institute of Technology reserves the right to distribute this thesis or dissertation

Printing note: If you do not wish to print this page, then select "Pages from: first page # to: last page #" on the print dialog screen

ABSTRACT

EVALUATION OF METHODS TO ACCOUNT FOR RELEASE FROM NANOFIBER SCAFFOLDS

by
Jennifer Moy

Electrospinning is a common technique utilized to form fibers from the micro- to nanometer range. Nanofibers form through electrospinning can be utilized as scaffolds since the fiber structures are similar to the structures within the extracellular matrix. Researchers use additives, such as growth factors, to help facilitate cell proliferation and function. Also, researchers are attempting to use electrospun fibers for drug delivery and as wound dressings since the electrospun fibers have high surface area to volume ratio. In both situations, the release of either the additive or the drug needs to be controlled so that the fibers would release the additive or drug in a desired manner. To understand the release from the electrospun fibers, researchers develop mathematical models that rely on the release data. Additionally, researchers utilize models based on Fick's second law of diffusion to predict release in cylindrical coordinates. This work aims to understand the release from electrospun fibers by finding the relationship between Fick's second law of diffusion and the mathematical models from experimental data. Three different release studies for electrospun fibers are investigated. Predicted mutual diffusion coefficients are developed so that the coefficients could be used for future predictive releases.

EVALUATION OF METHODS TO ACCOUNT FOR RELEASE FROM NANOFIBER SCAFFOLDS

by
Jennifer Moy

A Thesis
Submitted to the Faculty of
New Jersey Institute of Technology
in Partial Fulfillment of the Requirements for the Degree of
Masters of Science in Biomedical Engineering

Department of Biomedical Engineering

May 2014

APPROVAL PAGE

EVALUATION OF METHODS TO ACCOUNT FOR RELEASE FROM NANOFIBER SCAFFOLDS

Jennifer Moy

Dr. George L. Collins, Thesis Advisor Research Professor of Biomedical Engineering, NJIT	Date
Dr. Treena L. Arinzeh, Committee Member Professor of Biomedical Engineering, NJIT	Date
Dr. Bryan J. Pfister, Committee Member Associate Professor of Biomedical Engineering, NJIT	Date

BIOGRAPHICAL SKETCH

Author: Jennifer Moy

Degree: Master of Science

Date: May 2014

Undergraduate and Graduate Education:

- Master of Science in Biomedical Engineering,
  New Jersey Institute of Technology, Newark, NJ, 2014

- Bachelor of Science in Biomedical Engineering,
  New Jersey Institute of Technology, Newark, NJ, 2013

Major: Biomedical Engineering

Presentations:

Dung T. Le, George J. Ulsh, Jennifer W. Moy, and Maxwell A. McDermont, "ChitO_2-Clot™ A Novel Hemostatic & Oxygen Releasing Biomaterial," The TechQuest Awards, Newark, NJ, April 2013

Patents:

Ulsh, George, Ulsh, Dung, Moy, Jennifer, McDermott, Maxwell, Collins, George, and Cardenas, Jessica. 2014. System and method for hemostatic wound dressing. U.S. Patent Application 14165147, filed January 27, 2014. Patent Pending.

This thesis is in dedication to my parents and brother, who have supported me throughout the journey of earning this degree.
Without your support through the tough times, I would not be where I am today.
Thank you

ACKNOWLEDGMENT

I would like to thank Dr. George Collins, for allowing me to conduct this study while giving me advice throughout, and pulling it from the brink of defeat. I am thankful to Dr. Treena Arinzeh and Dr. Bryan Pfister for serving in the committee. I greatly appreciate Dr. Willis Hammond for allowing me to use the chemicals in his lab, for providing the crosslinkers used in this study, and for assisting me in finding solutions to unexpected problems. I like to specially thank Dr. Xueyan Zhang, for demonstrating the use of the cyro-scanning electron microscope, and for teaching me how to use scanning electron microscope. Thanks to Dr. Bruno A. Mantilla, John Palmieri, Fernando Arias, Jennifer M. Rochette, and Andrew Hollingsworth for listening to my countless iterations of my defense presentation. My eternal gratitude goes to Dung Thien Le, Gloria Portocarrero, and Lakshit Tripathi for allowing me to use their release studies from their electrospun fiber release systems. Without their help, this study would cease to exist. Thanks goes to all the members of the CHEN building for helping me both directly and indirectly. Lastly, I am grateful to my mother, Mae N. Moy, my father, Robert C. Moy, and my brother, James Y. Moy, for supporting me and giving me every opportunity to succeed.

TABLE OF CONTENTS

TABLE OF CONTENTS
(Continued)

TABLE OF CONTENTS
(Continued)

Chapter **Page**

LIST OF TABLES

LIST OF FIGURES

LIST OF FIGURES
(Continued)

Figure **Page**

CHAPTER 1

INTRODUCTION

1.1 Objective

In the evolving field of Tissue Engineering, researchers work to find ways of repairing and restoring damaged tissue by creating scaffolds that cells could adhere to and proliferate. Through fabricating scaffolds, researchers aim to mimic the extracellular matrix (ECM) so that the researchers could understand the environmental cues the cells sense and manipulate the cues in order to sustain the cells. To imitate the ECM, many researchers have turned to the technique of electrospinning biomaterials. The technique of electrospinning is appealing to researchers since the technique of electrospinning can create nanometer to micrometer diameter fibers that are similar in size to the structures in the ECM [1]. In addition to providing a structure similar to the cell's ECM, researchers have added additives to help facilitate cell proliferation and function. Researchers have electrospun fibers with growth factors so that the cells would interact directly with the growth factors to help sustain cell differentiation or growth. However, the concentration of the additives has to be controlled since cells may not favorably respond to the additive if the concentration is higher or lower than biological concentrations [2].

Additionally, the electrospun fibers can be used as a possible drug delivery device for continuous controlled release. Researchers have taken an interest in using electrospun fibers for drug release since the fibers have a high surface area to volume ratio and the drug could be added to the fibers by added the drug to the electrospinning solution prior to fiber fabrication. The researcher could control the release of the drug through

modifying the fibers so that the drug could be released at a therapeutic rate [3]. Despite the advantages of including drugs into electrospun fibers, the drug release from the electrospun fibers is not well understood. In many cases, the development of the drug release system is done through experimental testing without having a theoretical model to help predict the release of the drug prior to testing. The research reported here aims to evaluate mathematical models to account for the release of additives from electrospun fibers.

The objective of this research is to assess mathematical models to understand release of additives from electrospun fibers. In most studies on the release of additives from electrospun fibers, researchers measure the release of the additives and fit the data to a model based on fitting the empirical data to a statistical model [4]. However, the empirical model does not allow for predictions on release without having previous release data with the same conditions. Another mathematical that exists for release based on diffusion has been solved by Crank [5]. To assess which mathematical model would be better to predict release from electrospun fibers, the theoretical results were compared to experimental release data from three different cases. The first case was focused on the release of oxygen from chitosan fibers that contained an entrapped perfluorocarbon (PFC) for the purpose of creating a hemostatic wound dressing. Chitosan is natural biodegradable polymer that derives from the fungi and the exoskeleton of insects and crustaceans [6]. PFCs are fluorine substituted hydrocarbons capable of dissolving gases, such as carbon dioxide, oxygen, and nitrogen [7]. The second case focused on using release data that was obtained from a previous study on the release of sodium cellulose sulfate from electrospun fibers made of gelatin. The study was conducted by Gloria

Portacerreo and the methods used for fabricating the fibers will not be discussed in this thesis. The third case focused on the release of glucosamine sulfate from crosslinked gelatin fibers. Glucosamine sulfate is an amino sugar that is widely used as a daily supplement for relieving joint pain, improving joint strength, and strengthening bone [8]. Gelatin is a natural high molecular weight polymer that is formed through the hydrolysis of collagen. Since gelatin easily dissolves in water, the fibers had to be chemically crosslinked in order to prevent the chains of gelatin from dispersing in an aqueous environment [9]. For the first and third case, the fibers were electrospun with and without the additive to study the release of the additive from the fiber.

In this study, three different cases were considered for the release of an additive in order to compare the results to the mathematical models. For case one, the fibers were fabricated from a solution consisting of chitosan as the solute and a mixture of trifluoroacetic (TFA) acid and methylene chloride (MeCl) as the solvent. Additionally, perfluorotributylamine (PFTBA) was used as the perfluorocarbon additive. The chitosan fibers were neutralized in a solution of 100% ethanol and ammonium hydroxide in an one to one ratio in order to remove any remaining TFA. For the third case, the fibers were fabricated from a solution consisting gelatin and glucosamine sulfate dissolved in deionized water. Isosorbide bisepoxide (IBO) was added to the solution at various weight percents (wt%) in order to crosslink the gelatin fibers once the fibers were heat treated. In the two cases, the fibers were assessed for surface morphology. All three cases for assessed for the additive release. Only the gelatin fibers were assessed for swelling and degradation rate since crosslinked gelatin fibers can swell and degrade in an aqueous environment based on the level of crosslinking.

1.2 Background Information

1.2.1 Release Mechanisms

The release of an additive, or solute, from a solid matrix has been divided into three accepted types of controlled release, which are diffusion, swell, and chemical controlled release. For most systems employed in the pharmaceutical and biomedical practice, the release involves utilizing a combination of the release mechanisms. The solute can be included into the solid matrix by either entrapping the solute into the solid matrix or by covalently attaching the solute to the solid matrix. The release mechanism will depend on how the solute is included into the solid matrix and how the solid matrix degrades over the time period that the solute is being released [10]. Figure 1.1 is a comparison of the three categories of release mechanisms.

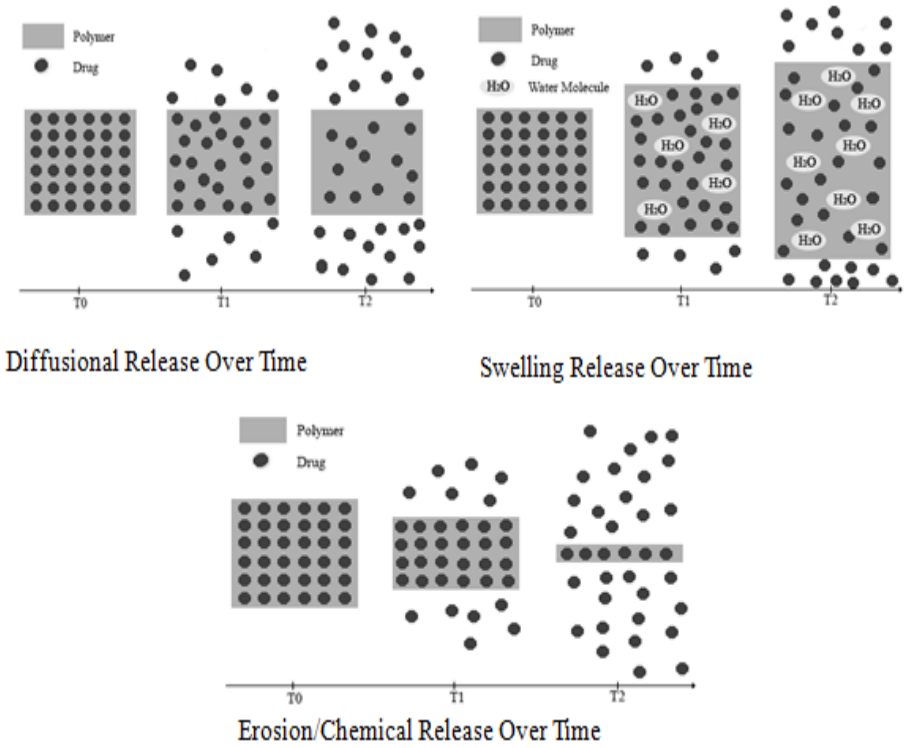

Figure 1.1 Comparison of diffusion, swell, and chemical controlled release over time.

1.2.1.1 Diffusional Release

Diffusional release occurs when the solute diffuses through the solid matrix while the solid matrix does not degrade. In addition, water does not enter the matrix faster than solute release. During diffusional release, the solute must enter the pores within the solid matrix and travel through the matrix based on a concentration gradient between the inside of the solid matrix and the outer environment. Once the solute reaches the surface of the solid matrix, the solute must undergo desorption from the solid matrix and enter the external medium where the solute travels to its intended target. The release rate can be predicted with Fick's second law of diffusion where the concentration gradient controls the rate of diffusion [10].

$$\frac{\partial \emptyset}{\partial t} = D_{12} \frac{\partial^2 \emptyset}{\partial x^2} \tag{1.1}$$

where

$\frac{\partial \emptyset}{\partial t}$ is the change in concentration gradient ($\partial \emptyset$) over a change in time (∂t)

$\frac{\partial^2 \emptyset}{\partial x^2}$ is the rate of change of the concentration gradient ($\partial \emptyset$) over the rate that the solute is traveling (∂x).

D_{ij} is the mutual diffusion coefficient for the solute (1) in the solid matrix (2), which can be to the self diffusion coefficients (shown in equation 1.2).

$$D_{12} = \left(\frac{D_1 x_2 + D_2 x_1}{RT}\right)\left(\frac{\partial \mu_1}{\partial ln x_1}\right)_{T,P} \quad (1.2)$$

where

D_1 and D_2 are the self diffusion coefficients of the solute and polymer respectively.

x_1 and x_2 are the mole fraction of the solute and the polymer respectively.

μ_1 is the chemical potential of the solute in the release system.

T is the temperature of the release system.

R is the universal gas constant.

In the case of pure diffusion from a solid matrix, the mutual diffusion coefficient represents the diffusion of a solute in a solid matrix. In most cases, the mutual diffusion coefficient is unknown. Attempts have been made in creating predictive models for estimating the mutual diffusion coefficient. However, the work is in its early phase and further work must be conducted before the solid-solid diffusion coefficient can be easily predicted [11].

1.2.1.2 Swell Release

Swell release occurs when the solid matrix transporting the solute is made from a hydrophilic material. Thus, water enters the solid matrix faster than the diffusion of the solute through the solid matrix that occurs for diffusion only release. As the water enters the solid matrix, the solid matrix's polymer chains relax and the entrapped solute can start traveling out of the matrix. Once the water completely enters the solid matrix, the solute

is released based on Fick's second law of diffusion (equation 1.1). For this system, the mutual diffusion coefficient is represented by the solute in a matrix system that is both solid and liquid. Fick's second law of diffusion only applies for when the polymer chains have fully relaxed and water has completely entered the solid matrix [10].

1.2.1.3 Chemical Release

Chemical or erosion release occurs when the solid matrix breaks down faster than the diffusion of the solute from the matrix. For chemical release, the solute can either be entrapped or covalently bonded to the matrix. The rate of solute release is controlled by the degradation rate of the solid matrix as the outer layer erodes away [10].

1.2.2 Mathematical Modeling

Various mathematical models have been utilized to describe the release of solutes from the solid matrix. Despite the wide variety of mathematical models, the most widely used model solute release is the power law since the power law can easily be obtained through curve fitting the experimental release data. The equation for the power law is below.

$$\frac{M_t}{M_\infty} = kt^n \tag{1.3}$$

where

$\frac{M_t}{M_\infty}$ is fraction of solute release.

t is the release time.

k and n are terms obtained through curve fitting.

The values for k and n are dependent on the diffusion rate of the solute from the solid matrix and the release mechanism respectively [4].

Other mathematical models that have been developed are based on the solutions of Fick's second law of diffusion. By solving Fick's law of second diffusion for a given geometry, the release of a solute can be found in respect to time. The equation for diffusional release from cylindrical coordinates was considered since the cylindrical geometry can be used to help account for the electrospun fiber's high surface area to volume ratio. The effect of changing the fiber diameter can easily be seen in cylindrical coordinates. The solute is assumed to diffuse from its original location where its embedded within the polymer chains to the outside of the fiber. In addition, the size of the solutes diffusion from the fiber are significantly smaller than the fiber's radius. The concentration of solute releasing from the other fibers is assumed to be not significant since the distance between the fibers are large in comparison to the size of the molecule. Thus, diffusional release from cylindrical coordinates was considered for the study.

To account for diffusion from cylindrical coordinates, Fick's second law of diffusion can be solved in cylindrical coordinates (as shown by figure 1.2), where the release from the cylinder of radius a will be one dimension radial release [12].

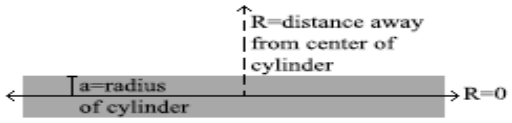

Figure 1.2 Cylindrical coordinates used for solving for solute release from cylinders.

The governing equation used to solve for solute release is based on equation 1.4.

$$\frac{\partial C}{\partial t} = D_{12}\left[\frac{\partial^2 C}{\partial r^2} + \frac{1}{r}\frac{\partial C}{\partial r}\right] \quad (1.4)$$

where

C is the concentration of the solute.

t is the time in which the release is occurring.

r is the radius of the cylinder.

D_{12} is the mutual diffusion coefficient for the solute in the solid matrix.

The system is assumed to be under perfect sink conditions, where the initial concentration of the solute in the external environment is zero. The solute is assumed to be evenly distributed from the center of the cylinder to the outer layer of the cylinder. The solute is assumed to have a constant concentration at the outer layer of the cylinder, where the concentrations do not have to equal each other [5]. The solution for Fick's second law under the given conditions is given in equation 1.5

$$\frac{M_t}{M_\infty} = \left(1 - \sum_{n=1}^{\infty} \frac{4}{a^2 \alpha_n^2} \exp\left[-D_{12} * \alpha_n^2 * t\right]\right) \quad (1.5)$$

where

$\frac{M_t}{M_\infty}$ is fraction of solute release.

a is the radius of the cylinder.

t is the time in which the release is occurring.

D_{12} is the mutual diffusion coefficient for the solute in the solid matrix .

$\propto_n$ is the positive zeros of the Bessel function on the zero order given as

$$J_o(a \propto_n) = 0 \tag{1.6}$$

The equation for diffusion release in cylindrical coordinates is not commonly used for understanding solute release since the mutual diffusion coefficient is often misinterpreted or assumed to be the diffusion coefficient of only the solute [12].

Both the power law and the equation for diffusional release in cylindrical coordinates can be used to calculate for the fraction of solute release. In an attempt to find the relationship between the diffusion release in cylindrical coordinates and the power law equation, the diffusion release in cylindrical coordinates has been expanded for short time behavior. The expansion is given below as equation 1.7.

$$\frac{M_t}{M_\infty} = 4\left[\frac{D_{12}t}{\pi a^2}\right]^{1/2} - \pi\left[\frac{D_{12}t}{\pi a^2}\right] - \frac{\pi}{3}\left[\frac{D_{12}t}{\pi a^2}\right]^{3/2} + \ldots \tag{1.7}$$

where

$\frac{M_t}{M_\infty}$ is fraction of solute release.

a is the radius of the cylinder.

t is the time in which the release is occurring.

D_{12} is the mutual diffusion coefficient for the solute in the solid matrix.

By expanding the solution for diffusional release in cylindrical coordinates for the first three terms, the terms in the equation start to resemble the terms in the power law. The value of k can be found by assuming that the first term of the expansion can represent the

power law for n=0.50. With the assumption, the value of k within the power law ends up equaling equation 1.8.

$$k = 4\left[\frac{D_{12}}{\pi a^2}\right]^{1/2} \tag{1.8}$$

where

$\frac{M_t}{M_\infty}$ is fraction of solute release.

a is the radius of the cylinder.

D_{12} is the mutual diffusion coefficient for the solute in the solid matrix.

Thus, the k value in the power law is accounting for the complexity of the mutual diffusion coefficient and the effects of the radius during diffusion. The relationship between k and the first term of the expansion of the diffusional release in cylindrical coordinates is only valid for the first 15 to 20% of the solute release since the mutual diffusion coefficient varies with time [6].

1.2.3 Electrospinning

Electrospinning is an electrohydrodynamic technique that utilizes the ability to charge a solution in a needle so that the solution can overcome its surface tension and form micro to nanoscale fibers. The solution can vary from polymers dissolved in a solvent to melted forms of raw materials that can be pumped through a needle at a constant flow rate. The solution is charged as it travels through the needle by either having a high power direct current voltage supply attached to the outer part of the needle or by inserting a probe

directly into the solution. As the charge solution is pumped through the needle, the solution forms a bead at the needle tip. When the charge in the solution is strong enough to overcome surface tension, the bead forms into a Taylor cone, or a cone shape bead where the repulsion of the charge solution is higher than the surface tension. The solution forms fibers as the charged solution travels from the Taylor cone and hits the grounded collector plate (as depicted in figure 1.3). The repulsion of the charges within the solution causes the fibers to elongate as the solution travels from the needle tip towards the collector plate. The fibers are further elongated when the solution undergoes a whipping motion as the solution travels towards the collector plate from the instabilities in the electric field formed between the needle tip and the collector plate. The solvent of the solution evaporates as the solution travels to the collector plate so that the fibers formed on the collector plate. After the fibers are collected from the collector plate, the fibers may need to be neutralized to remove any remaining acids or bases that did not evaporate from the solution before the formed fibers collect on the collector plate. The fibers can range from the micrometer to nanometer range depending on the electrospinning parameters [13].

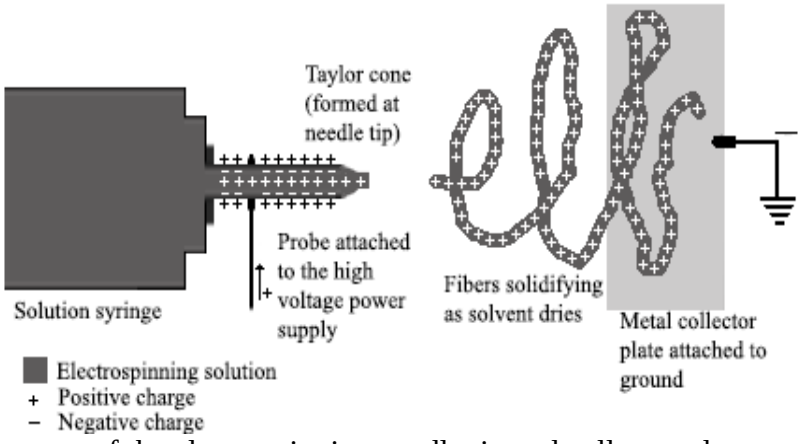

Figure 1.3 Close up of the electrospinning needle tip and collector plate.

The electrospinning parameters can be divided into three separate categories consisting of solution parameters, spinning parameters, and ambient parameters. Solution parameters consists of solution viscosity, molecular weight of the polymer, and the type of solvent used to dissolve the polymer. The electrospinning solution has to have a low enough viscosity so that the solution can be pumped through the needle tip. However, the solution must have a high enough viscosity so that the polymer chains can form enough entanglements. If the level of polymer chain entanglement is too low, the solution will form beads instead of fibers during electrospinning because the polymer chains are too short to form a continuous fiber after the solvent evaporated from the solution. The spinning parameters are the needle gauge, the applied voltage at the needle tip, the flow rate applied to the solution syringe, and the needle tip to collector plate distance. The needle gauge will affect the size of the Taylor cone that forms at the needle tip. The applied voltage and flow rate are dependent on each other since the flow rate must be high enough to replenish the solution at the needle tip while the applied voltage will determine the rate at which the solution leaves the needle tip to form fibers. The needle tip to collector plate distance affects the strength of the electric field between the needle tip and collector plate. Additionally, the needle tip to collector plate distance can be altered to change the amount of drying time for the solvent to evaporate from the fibers. Lastly, the ambient parameters consist of temperature and humidity. The temperature alters the viscosity of the solution while the humidity increases the drying time for the solution. In most situations, only the solution and spinning parameters can be altered. However, the ambient parameters can be changed depending on the electrospinning set up.

The electrospinning set up consists of a syringe containing the solution for electrospinning, a needle attached to the syringe, a system for controlling the flow rate of the syringe containing the solution, a high power voltage source capable of charging the needle, and a metal collector plate that is connected to a ground. Additional equipment may be required for the electrospinning set up depending on the type of solution that is being electrospun. The electrospinning set up utilized for the study is depicted in figure 1.4. A heating set up has been created so that solutions required to be at temperatures higher than the room temperature could be heated during the duration of the electrospinning process. The solution syringe is enclosed in a heating containment so that the electrospinning hood does not have to be completely heated. To heat the solution, hot air is pumped into the containment by passing air from an air compressor through a heated metal pipe that is attached to insulated tubing that leads to the heating containment. A dehumidifier and humidifier has been added to the electrospinning set up (not depicted in figure 1.4) to help control the humidity within the electrospinning hood.

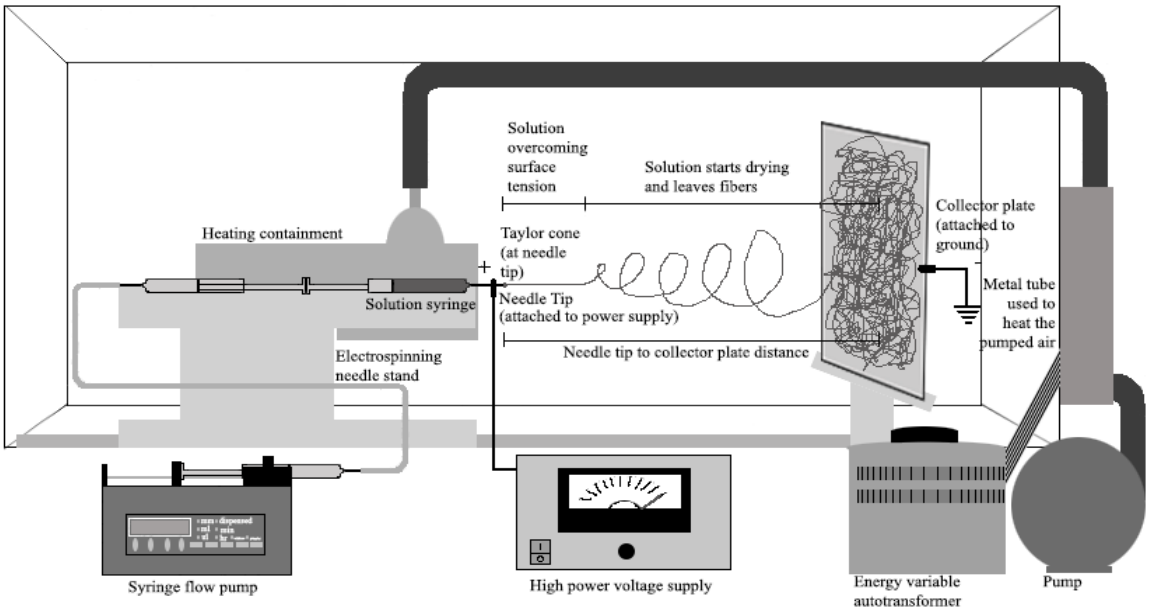

Figure 1.4 Schematic of the electrospinning unit.

1.2.2.1 Solute Inclusion in Electrospinning

Solutes can be introduced into electrospun fibers through three major ways, which are post spinning, electrospinning the solution as a blend, and core shell spinning. One method may be favorable over the other methods depending on the available electrospinning set up and the chemicals utilized during the electrospinning process. The mechanism for the solute release will depend on how the solute is introduced into the electrospun fibers [3]. Figure 1.5 is a comparison of the three ways of including the solute into the electrospun fibers.

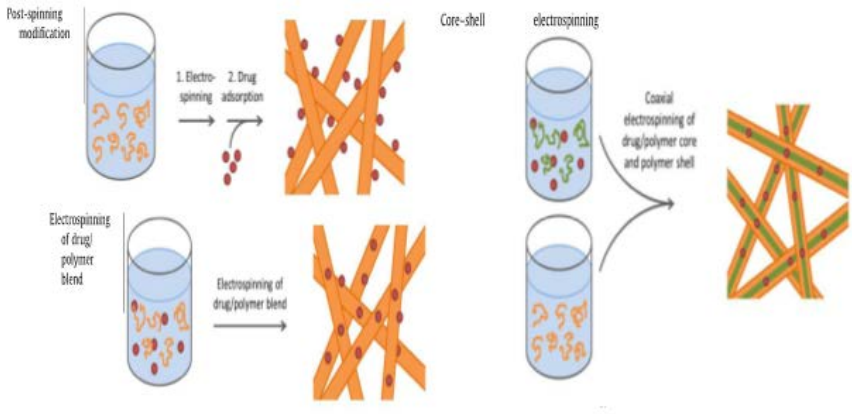

Figure 1.5 Comparison of methods used to introduce solute into electrospun fibers.
Source: [3].

For post spinning, the electrospun fibers are fabricated before the solute is added to the system. The solute is added to the fibers through adsorption of the solute to the electrospun fibers. Post spinning modification of the solute to the fibers allows for prolonged solute release since the solute would be covalently bonded to the fibers. However, the release from the fibers is harder to predict since the release is dependent on the cleavage of the covalent bonds between the solute and fiber and the degradation rate of the electrospun fibers [3].

For core shell electrospinning, two solutions are electrospun together where the solution of the solute and the polymer and the solution of the polymer by itself would be coaxially electrospun. Through the use of core shell electrospinning, the fibers would have an inner core containing the solute and the outer layers would contain only the polymer solid matrix. Core shell electrospinning allows for a higher control of solute release since the solute must first travel through the outer layer of the polymer before being released [3].

For electrospinning the solute as a blend, the solute is introduced into the electrospinning solution before electrospinning. Thus, the formed fibers would have the solute distributed throughout the electrospun fibers. By adding the solute to the electrospinning solution, the solute release would be dependent on the characteristics of the polymer matrix and the interactions between the solute and polymer [3].

1.2.4 Chitosan

Chitosan is a natural polysaccharide derived from chitin, which can be found in fungi, the exoskeleton of insects, and the shells of crustaceans. Researchers utilized chitosan in a variety of biomedical applications since chitosan can be easily obtained from an abundant renewable resource and is known to be biodegradable and antimicrobial [6]. Additionally, researchers used in the fabrication of wound dressings since chitosan has both intrinsic hemostatic and antimicrobial properties. Since chitosan can have protonated amine groups, chitosan can attract negatively charged residues on red blood cell membranes to cause the clumping or agglutination of red blood cells. Also, chitosan can absorb fibrinogen and plasma proteins to enhance the agglutination process [14]. The mechanism

for how chitosan inhibits microbial growth is currently unknown [6]. The structure of chitosan is given in figure 1.6.

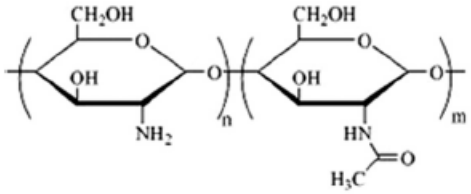

Figure 1.6 Structure of chitosan.

Source: [15].

1.2.4 Perfluorotributylamine

Perfluorotributylamine (PFTBA) is a perfluorocarbon (PFC), which is a group of fluorine substituted hydrocarbons. PFCs have a low surface tension in comparison to the hydrocarbon counterparts since fluorine has a low interactions between each other versus hydrogen, which leads to low cohesive energies in the PFC. The low interactions between the fluorinated side chains allows PFCs to dissolve gases with high efficiency [7]. The gases dissolved into the PFCs are bounded to the PFC by van der Waals bounding. Since the gases are held to the PFCs by weak bonds, the gases can easily be released from the PFCs [16]. The chemical structure of PFTBA is given below in figure 1.7.

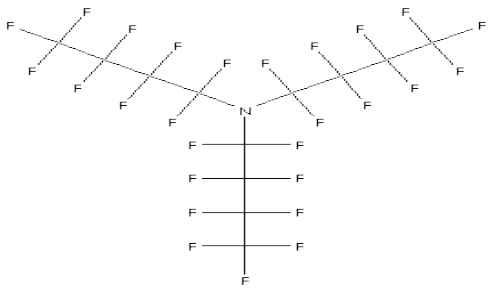

Figure 1.7 Chemical structure of PFTBA. Unlike the hydrocarbon structure, the side chains consist of fluorine.

Source: [17].

The amount of dissolved gas in PFCs follows Henry's law, where the concentration of the dissolve gas depends on the partial pressure of the gas and the Henry's constant for the gas. By loading the PFC under high oxygen concentration, the PFC can unload the dissolved oxygen up to 90% of the dissolved oxygen when in low oxygen concentrations [7]. Henry's law for oxygen is given in equation 1.9.

$$P = C * k_h \tag{1.9}$$

where

P is the partial pressure of oxygen in units of atm.

C is the concentration of oxygen in units of mol/L.

k_h is Henry's constant for oxygen, which is equal to 769.23 (L*atm)/mol [18].

Since PFCs have a high solubility for oxygen, PFCs have been used for use for various applications, such as liquid ventilation, organ preservation, blood substitute, and an oxygen carrier for cell and tissue culture. However, PFCs cannot be directly used in an aqueous environment since PFCs are immiscible in water. Thus, PFCs are prepared as an emulsion to prevent the PFC from separating away from water when the PFC is injected into an aqueous environment [7].

1.2.5 Gelatin

Gelatin is a natural biopolymer formed through the partial hydrolysis of collagen, which is one of the most abundant structural protein within the human body. By denaturing

collagen, the collagen protein loses the triple helical three-dimensional structure and becomes soluble in water [19]. Since gelatin is derived from collagen, gelatin has been used in various biomedical and pharmaceutical applications.

The properties of gelatin changes depending the process utilized to extract collagen. Type A gelatin comes from collagen that has been gathered from a source that was pretreated with an acid. Type B gelatin comes from a collagen source that had undergone an alkaline process that targets the amide groups of asparagine and glutamine. The process hydrolyses the amide groups and converts them into carboxyl groups, which changes the balance between amide and carboxyl groups. The reduction in amide groups causes the gelatin formed after denaturing the collagen to have an overall negative charge. Depending on the release application, either gelatin type A or type B may be more favorable since the charge on the gelatin can be used as a way of providing sustained release. By having the additive of the opposite charge to the gelatin, the additive release rate would decrease since the additive would have to overcome the attractive force between itself and gelatin before diffusing through the structure and releasing into the surrounding environment [20].

1.2.6 Glucosamine Sulfate and Glycosaminoglycans

Glucosamine sulfate is a monosaccharide that is a precursor of glycosaminoglycans. As a monosaccharide, glucosamine sulfate is utilized in the biosynthesis of glycosaminoglycans, which are used for the production of aggrecans and other proteoglycans present in cartilage. The structure of glucosamine sulfate is given in figure 1.8.

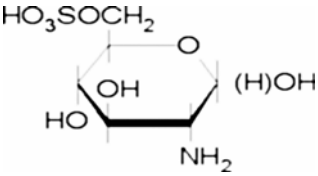

Figure 1.8 Chemical structure of glucosamine sulfate.

Source: [21].

Glycosaminoglycans are linear polysaccharides that are made from uronic acid and amino sugars. Within the body, glycosaminoglycans performs a variety of functions, which includes osmotically attracting water to help maintain the hydrostatic pressure in connective tissue, and interacting with proteins on cell surfaces to interact with the biological environment. The functionality of the glycosaminoglycan changes depending on the repeating disaccharide of the uronic acid and amino sugar. For instance, highly sulfated glycosaminoglycans, such as chondroitin sulfate, possess a negative charge that depends on the density and position of the sulfate group, which helps in attracting positively charged proteins. The structure of chondroitin sulfate is given in figure 1.9 as an example of a glycosaminoglycan.

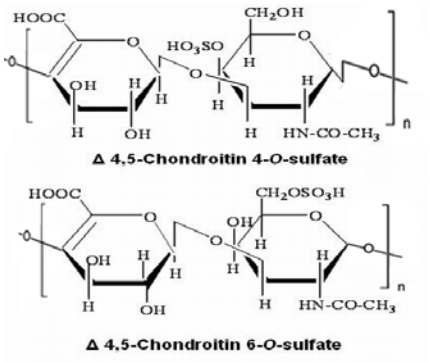

Figure 1.9 Chemical structure of chondroitin sulfate. The top chemical structure shows the sulfate group bonded in the forth position while the bottom chemical structure shows the sulfate group in the sixth position.

Source: [22].

1.2.7 Chemical Crosslinking

Crosslinking is a technique used to maintain structures by adding additional chemical bonds. Common chemical crosslinking agents utilized for crosslinking gelatin includes glutarldehyde, epoxy compounds, carbodiimides, and acyl azide. Additionally, crosslinking can be done through the use of heating, drying, and irradiation. The degree of crosslinking will vary depending on the technique used for crosslinking. For the study, isosorbide bisepoxide (IBO) is used. Since IBO is an epoxy compound, IBO will form bonds with the amine groups of gelatin. Depending on the amount of amine groups present in gelatin will determine the maximum amount of crosslinking that can be done to crosslink gelatin [23].

CHAPTER 2

MATERIALS AND METHODS

2.1 Materials

Medium weight chitosan, gelatin type B from bovine skin (75 bloom), glucosamine sulfate, sodium formate, and 1,9 dimethylmethylene blue were obtain from Sigma Aldrich. PFTBA (85%) was obtained from Matrix Scientific. Trifluoroacetic acid, methylene chloride, absolute ethanol, ammonium hydroxide, and formic acid were purchased from Fisher Scientific. The Isosorbide bisepoxide utilized in the study was synthesize by Dr. Willis Hammond (New Jersey Institute of Technology, Department of Biomedical Engineering, Newark, NJ/ Batch 3 169/66, Date May 13th 2011).

2.2 Electrospinning Unit

The electrospinning set up utilized in the study is shown in figure 1.2. The unit consists of a syringe pump (New Era pump systems Inc), a high power voltage source (Gamma High Voltage Research Power Supply Model # 5560-0.38), a energy variable autotransformer (Staco Energy Variable Autotransformer), and a pump (Labcono motor-catalog no 50054). The other equipment in the electrospinning unit were created specifically for the electrospinning set up.

2.3 Fabrication of Chitosan Fibers Infused with Perfluorotributylamine

2.3.1 Solution Preparation

A 5.6 wt% chitosan solution was prepared by adding chitosan powder into a solvent consisting of a volume ratio of 80 to 20 TFA to MeCl. Briefly, the TFA and MeCl were measured and mixed together in a graduated cylinder and poured into a glass container. Chitosan was measured out based on being seven weight to volume percent (7 wt/vol%) of the TFA and MeCl mixture based on the following equation:

$$\text{wt/vol chitosan} * \text{volume of 80 to 20 TFA to MeCl} = \text{weight of chitosan} \quad (2.1)$$

After measuring the chitosan, the chitosan was added to the TFA and MeCl mixture and the solution was left to stir on a magnetic heated stirring plate at 60^{o}C for one hour.

While the chitosan solution was set to stir on the heated stirring plate, the PFTBA was loaded with oxygen through bubbling air into the PFTBA liquid. Briefly, the volume of PFTBA for the electrospinning solution was measured in a ratio of 1 to 10 PFTBA to chitosan solution and was added to a glass vial. Air from an air compressor was bubbled into the PFTBA for five minutes. The oxygenated PFTBA was added to the chitosan solution once the chitosan solution has stirred for an hour. The solution was left to stir at 60^{o}C for an additional five minutes.

2.3.2 Electrospinning

Prior to solution preparation, the hood containing the electrospinning unit was brought to 25% humidity with the use of a humidifier. A plastic tube was attached to the humidifier so that the water vapor from the humidifier could be fed into the electrospinning hood without having the humidifier in the hood during electrospinning. Additionally, the heating containment was set up as shown in figure 1.2 but without having the solution syringe in place so that the system could reach the desired temperature. The energy variable autotransformer was set to output 60% of the maximum voltage output so that the air pumped to the heating containment would reach 60^{o}C.

Once the prepared chitosan solution containing PFTBA was ready, the solution was fed into a 10mL disposable syringe and an 12 gauge needle was fitted onto the syringe. The syringe was inserted into the electrospinning needle stand and the heating containment was slipped over the needle stand. The needle stand was moved so that the needle tip would be 30 cm away from the collector plate that was attached to ground. Afterwards, the syringe pump was set to pump at 2 ml/hr and a 30 to 35 kV voltage was applied to the needle. Throughout the process, the humidity was kept at 25-35% and the temperature of the solution was kept at above 60^{o}C so that the solution would not form a gel during electrospinning. The temperature of the rest of the unit was kept at room temperature.

Table 2.1: Parameters for Electrospinning Chitosan Fibers Infused with PFTBA

Parameter	
Needle Gauge	12 Gauge
Voltage	30-35 kV
Flow Rate	2 ml/hr
Needle Tip to Plate Distance	30 cm
Humidity	25-35%
Heat	>60^{o}C

Following electrospinning, the electrospun fibers were collected off of the collector plate and placed into a solution containing an one to one ratio of 100% ethanol to ammonium hydroxide. The fibers were kept in the solution for 30 minutes in order to neutralize the remaining TFA that may not have evaporated from the fibers during electrospinning. After the 30 minutes, the fibers were placed into deionized water for an additional 30 minutes. The fibers were removed from the deionized water and placed into deionized water for another 30 minutes before rinsing the fibers and drying the fibers in an oven at 30^{o}C until the fibers were dried. The same procedures were applied for creating chitosan fibers without PFTBA except additional heat was not applied to the solution during electrospinning.

2.4 Fabrication of Gelatin Fibers Infused with Glucosamine Sulfate

2.4.1 Solution Preparation

A 30 wt% gelatin solution was prepared by adding gelatin to deionized water that either contained glucosamine sulfate at a concentration of 35 μg per ml or contained no glucosamine sulfate. The solutions were created by measuring weight of the deionized

water either containing or not containing the glucosamine sulfate and calculating the total weight by the following equation.

$$\text{wt\% Component A} + \text{wt\% Component B} + \text{wt\% Component C+...} = 100 \quad (2.2)$$

By manipulation equation 2.2, the weight percent of deionized water in the solution can be calculated since the weight percent of gelatin and the crosslinker were set by the researcher. With the calculated weight percentage of the deionized water, the total weight of the solution can be calculated with the following equation.

$$\text{Total Weight} * \text{wt\% Component A} = \text{Weight of Component A} \quad (2.3)$$

After the total weight of the solution was calculated, weight of the gelatin and the weight of the crosslinker were calculated by equation 2.3. The gelatin was weighed out and added to the deionized water. The gelatin solution was heated at 60^{o}C and stirred for fifteen minutes or until the gelatin has dissolved in the solution. Ten minutes before using the solution for electrospinning, the crosslinker was added to the solution through adding drops of the crosslinker into the solution as its being weighed. The solution was returned to heat and stirred for another ten minutes. The solutions used for electrospinning are listed in table 2.2.

Table 2.2: Solutions Prepared for Electrospinning Gelatin

Solution Type	**Weight Solvent** g	**Weight Glucosamine Sulfate** mg	**Weight Crosslinker** g	**Weight Gelatin** g
30 wt% Gelatin in Deionized water	4.87±0.05	None	None	2.09±0.05
30 wt% Gelatin in Deionized water with 3 wt% IBO	2.07 ±0.005	None	0.09 ±0.005	0.92±0.005
30 wt% Gelatin in Deionized water with 5wt% IBO	1.99±0.005	None	0.15 ±0.005	0.92±0.005
30 wt% Gelatin in Deionized water with 7wt% IBO	2.02 ±0.005	None	0.23 ±0.005	0.96±0.005
30 wt% Gelatin in GS/Deionized water	2.02±0.005	70±0.5	None	0.87±0.005
30 wt% Gelatin in GS/ Deionized water with 3wt% IBO	2.00±0.005	70±0.5	0.10±0.005	0.90±0.005
30 wt% Gelatin in GS/ Deionized water with 5wt% IBO	1.99±0.005	70±0.5	0.17±0.005	0.93±0.005
30 wt% Gelatin in GS/ Deionized water with 7wt% IBO	2.00±0.005	70±0.5	0.22±0.005	0.96±0.005

2.4.2 Electrospinning

Prior to solution preparation, the heating containment was set up as shown in figure 1.2 but without having the solution syringe in place so that the system could reach the desired temperature. The energy variable autotransformer was set to output 70% of the maximum voltage output so that the air pumped to the heating containment would reach 81^{o}C. The heating containment was kept at a high temperature to prevent the solution from forming a gel in the syringe and in the syringe since gelatin forms a solid at room temperature.

Once the solution was ready to be electrospun, the solution was fed into a 10mL disposable syringe and an 12 gauge needle was fitted onto the syringe. The syringe was inserted into the electrospinning needle stand and the heating containment was slipped over the needle stand. The needle stand was moved so that the needle tip would be 14 cm away from the collector plate that was attached to ground. Afterwards, the syringe pump was set to pump at 2 ml/hr. For the solution containing glucosamine sulfate and no crosslinker, the flow rate was set 5 ml/hr. A voltage of 26 to 27 kV was applied to the needle. Throughout the process, the humidity was kept at 10-12% and the temperature of the solution was kept at above 60^{o}C so that the solution would not form a gel during electrospinning. The temperature of the rest of the unit was kept at room temperature. The humidity was kept below 12% since having a higher humidity prevented the fibers from drying as they collected on the collector plate.

Table 2.3: Parameters for Electrospinning Gelatin Fibers Infused with Glucosamine Sulfate

Parameter	
Needle Gauge	12 Gauge
Voltage	26-27 kV
Flow Rate	2-5 ml/hr
Needle Tip to Plate Distance	14 cm
Humidity	10-12%
Heat	>60^{o}C

Following electrospinning, the fibers were removed from the collector plate and wrapped in aluminum foil. The collected fibers were then placed into an oven (Symphony^{TM} VMR oven) at 130^{o}C for two hours. The fibers were heated in order to remove the remaining moisture and to provide the necessary heat for crosslinking the

fibers. After two hours, the fibers were removed from the oven and stored in wax paper until utilized for testing. The solution containing glucosamine sulfate were made in triplicate for the release study.

2.5 Film Fabrication

Films were casted with solutions containing higher concentrations of glucosamine sulfate in order to determine the release of glucosamine sulfate since the concentration of glucosamine sulfate may not be detectable with the dye used in the proteoglycan assay. As a control, films were casted with solutions containing sodium cellulose sulfate. Sodium cellulose sulfate has a similar structure to chondroitin sulfate and is known to react with dyes used in glycosaminoglycan assays. Since a limited amount of glucosamine sulfate was available, only one film was casted for glucosamine sulfate. The films were later used for staining for release studies.

The solutions were created so that the final film would have 12.5 wt% of either glucosamine sulfate or sodium cellulose sulfate. The weight percent of the crosslinker was set to either 0 wt% IBO or 12.5 wt% IBO. The weight percent of gelatin determined based on equation 2.2. The total weight of the films was calculated using equation 2.3 based on the set weight of 2.6 mg of glucosamine sulfate and the film having 12.5 wt % glucosamine sulfate. After the total weight of the film components was calculated, weight of the gelatin and IBO were calculated by equation 2.3. The glucosamine sulfate/sodium cellulose sulfate, gelatin, and IBO were measured and 1 gram of water was added to mix the mixed together in an aluminum weigh boat. The solution was heated at 60^{o}C and stirred with a needle tip until the components of the solutions dissolved. The solution was

spread to coat the surface of the weigh boat and the casted film was placed into the oven at 130^{o}C for thirty minutes to allow the water to dry from the film and to allow the crosslinker to crosslink with gelatin. The films were left in the weigh boats for late use. The solutions used for film casting are listed in table 2.4.

Table 2.4: Solutions Prepared for Casting Films

Solution Type	**Weight Solvent** g	**Weight Glucosamine Sulfate or Sodium Cellulose Sulfate** mg	**Weight Crosslinker** mg	**Weight Gelatin** mg
75 wt% gelatin with 12.5 wt% glucosamine sulfate and 12.5 wt% IBO	1.0250±0.0002	2.6±0.2	2.6±0.2	20.5±0.2
75 wt% gelatin with 12.5 wt% sodium cellulose sulfate and 12.5 wt% IBO	1.0150±0.0002	4.0±0.2	0	28.0±0.2
87.5 wt% gelatin with 12.5 wt% sodium cellulose sulfate	1.0211±0.0002	4.0±0.2	4.9±0.2	24.8±0.2

2.6 Material Characterization

2.6.1 Swell Test

To determine if the electrospun fibers were sufficiently crosslinked as well as how fast the gelatin fibers swell, samples from the electrospun fibers were utilized in swelling tests. The samples were taken from the electrospun fibers that do not contain glucosamine sulfate since the inclusion of glucosamine sulfate should not affect the uptake of water by the electrospun fibers. The fibers' swell rate will affect the assumptions used in predicting the glucosamine sulfate release.

A sample weighing between 0.0015 grams to 0.0059 grams were removed from the scaffolds containing 0 wt%, 3 wt%, 5 wt%, or 7 wt% crosslinker. The samples were weighed and placed onto separate Petri dishes. A preset intervals, each sample was picked up and dipped into a beaker containing deionized water. After being dipped in the water, the sample was placed back onto the Petri dish so that the excess water could be removed through five minutes of air drying before weighing the sample. A minute before weighing the sample, any remaining water was blotted away. The process was repeated over the course of an hour in order to determine if the fibers continued to swell. The swell ratio was calculated with the following equation.

$$Swell\ Ratio = \frac{W - W_o}{W_o} * 100 \tag{2.5}$$

where

W is the weight of the swollen sample.

W_o is the weight of the initial sample before swelling

2.6.2 Lyophilization

Since gelatin fibers swell when placed into an aqueous environment, the fiber diameters would increase. By increasing the fiber diameter, the rate of diffusion of the solute would change. Additionally, the pores that the solutes can diffuse out of change since the polymer chain entanglements within the swollen fibers relax. In order to account for the change in fiber diameter, the swollen fibers would have to be lyophilized, or freeze dried, so the diameter of fibers could be measured.

The unit used for lyophilization was created from the use of a refrigeration unit (DSC Cooling Unit- Perkin-Elmer), a vacuum pump (Becker Oil Less Vacuum Pump V 4.10) capable of creating pressure below 0.006 atm, a Styrofoam box, a beaker, isopropyl alcohol, a ring stand, a universal 3 prong clamp, a glass condenser, a round bottom flask to hold the sample, and a temperature gauge for measuring temperature of the isopropyl alcohol used to chill the sample holder. The unit set up is displayed in figure 2.1. The lyophilization unit works by placing the sample into the round bottom flask and attaching the flask to the condenser. The condenser is attached to the ring stand with the use of the prong clamp and the condenser is lowered into the Styrofoam box containing the beaker filled with isopropyl alcohol. The beaker was packed into place with Styrofoam so the beaker would not move from the top of the refrigeration unit's chilling component. By having the beaker on the chilling component, the isopropyl alcohol chills down to the temperature that the chilling component can output. Since the refrigeration unit can chill down to -87^{o}C and isopropyl alcohol remains in its liquid phase, only the water in the sample would freeze when the sample holder is submerged in the isopropyl alcohol. The refrigeration unit is turned on so the sample can be frozen. Once the sample is frozen, the tube attached to the vacuum pump is attached to the condenser and the vacuum pump is turned on. The lyophilization unit is left on for several hours to a day depending on the size and the amount of water in the sample so that the ice can be sublimated and drawn away from the sample through the vacuum. Once freeze drying is complete, the vacuum pump and refrigeration unit are turned off and the sample is removed.

Figure 2.1 Lyophilization unit setup.

For scanning electron microscopy (SEM), the samples have to be dried. To prepare the swollen samples to be imaged, samples from a randomly selected 3 wt%, 5 wt%, and 7 wt% crosslinked fibers containing glucosamine sulfate were taken and swollen in 6 ml of deionized water. After several hours to several days have passed, the samples were removed from the water and spread out onto aluminum foil. The samples were flattened out to help increase the surface area, which would help decrease the chilling time. Additionally, the samples must be flat in order to get a clean image with the SEM. Afterwards, the samples were inserted into the round bottom flask and the flask was attached to the condenser. Then, the condenser was repositioned on the ring stand so that the flask would be submerged in the isopropyl alcohol. The refrigeration unit was turned on and allowed to chill the isopropyl alcohol to -80^{o}C. The vacuum pump was attached to the condenser and the pump was turned on after the sample was allowed to

freeze for a half hour. The system was left to run for 20 hours before the system was turned off and the samples were removed for use in the SEM.

2.6.3 Scanning Electron Microscopy

Scanning electron microscopy (SEM) is a high resolution microscopic method for imaging the external morphology of conductive samples under vacuum. The SEM develops an image by bombarding the sample surface with electrons and the backscattered and secondary electrons' energies are measured to create an image of the surface in the micro to nanoscale. Additionally, X-ray fluorescence photons, Auger electrons, and other photons of various energies can be detected for creating an image of the sample surface [24].

Samples were first dried to remove any excess moisture since the moisture would interfere in the SEM imaging. Conductive tape was applied to standard SEM pin stubs and small portions of the electrospun fibers were flattened out onto the conductive tape. The samples were carbon coated by a sputter coater (BAL-TEC MED 020 Coating System) in order to make the samples conductive. After coating the samples, the samples were used for SEM imaging.

2.7 Release Studies

2.7.1 Oxygen Reading

Measurements of oxygen release from the electrospun chitosan fibers infused with PFTBA were conducted with an oxygen probe that is designed to detect the concentration of dissolved oxygen in water. The oxygen probe used for the release study was the

Vernier optical dissolved oxygen probe, which is capable of detecting oxygen concentrations in water in units of mg/L. The probe is capable of detecting dissolved oxygen (DO) in the 0 to 20.0 mg/L range and the system is capable of compensating changes in oxygen based on differences in temperature and pressure [25]. The oxygen probe is attached to a LabQuest 2 unit used to gather the oxygen concentration readings. The data collected in LabQuest 2 can be transferred to a computer in either a text or Excel document. The image of the probe is shown in figure 2.2.

Figure 2.2 Vernier optical DO probe.
Source: [25].

In the experiment, the electrospun chitosan fibers infused with PFTBA were placed in deoxygenated water and the oxygen released from the fibers was detected by the oxygen probe. First, deionized water is poured into a beaker. The beaker is placed into a glove bag along with the oxygen probe, LabQuest unit, and the electrospun chitosan fibers infused with PFTBA. The glove bag is attached to a tube leading to a nitrogen cylinder. The glove bag is partially sealed off to allow air to escape the bag while its being filled with nitrogen gas. After the glove bag is expanded, the bag is sealed off and the tube leading to the nitrogen gas is placed into the water to bubble the nitrogen gas into the water in order to deoxygenate the water. The oxygen probe is used to monitor

the oxygen concentration in the water until the oxygen concentration levels off. Afterwards, the nitrogen gas is turned off. The electrospun chitosan fibers infused with PFTBA is placed into the deoxygenated water and oxygen probe is used to stir the water as the oxygen concentration data is collected. The setup of the oxygen reading is shown in figure 2.3.

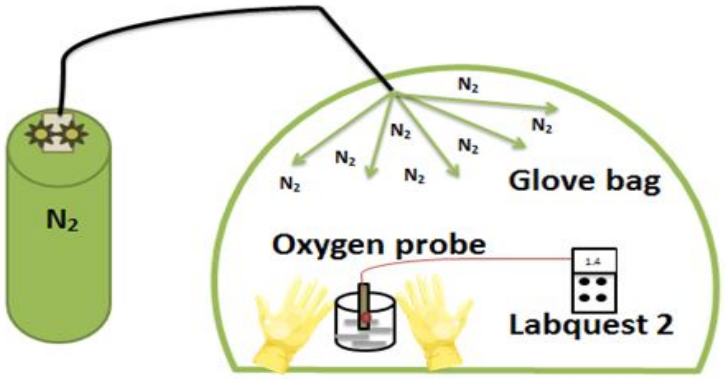

Figure 2.3 Oxygen release setup.

Source: [26].

2.7.2 Proteoglycan Assay

Quantification of total sulfated glycosaminoglycans is commonly performed with the use of 1,9-dimethylmethylene blue (DMMB) dye at a pH of 3.0. DMMB is a cationic dye that changes from a deep blue color to a violet pink color when in the presence of a sulfated glycosaminoglycan [27]. The DMMB is known to react by binding to the ionized sulfate and carboxyl groups present in the glycosaminoglycan chains [28]. The absorbance of the dye to glycosaminoglycan is linearly correlated to the concentration of the glycosaminoglycan from 0 to 100 μg/ml. Depending on the purity of the dye, the absorbance can be read at either 525 nm [28] or 595 nm [27].

The DMMB dye utilized for the assay was prepared using the method discussed by Enobakhare et al. Briefly, 11 mg of DMMB powder was added to 2.5 mL of absolute ethanol. The dye was diluted to 400 mL with distilled water and 1 g of sodium formate was added to the dye. The dye was adjusted to a pH of 3.0 with the use of formic acid. After adjusting the pH, the dye was diluted to a final volume of 500 mL. The dye was stored in a brown bottle and kept at room temperature where it would be stable for at least 2 months [27].

To test the dye, a standard curve was created in a 96 well plate by using the stock solution used to electrospin the gelatin fibers infused with glucosamine sulfate. The stock solution was serial diluted and the dye was used to cut the concentration of glucosamine sulfate in the standards in half. The standards used to make the standard curve were duplicated to account for variations when creating the standard solutions. After creating the standard curve, the 96 well plate was read with a microplate spectrophotometer (Molecular Devices Emax) at an absorbance of 650 nm since the microplate reader did not have a filter for 525 nm nor 595 nm.

For the release assay, the a sample from each electrospun gelatin fibers infused with glucosamine sulfate was weighed and inserted into a glass vial. 2 mL of deionized water was added to each vial and the vials were capped. After every hour, a 100 μl aliquot from each sample was taken to be used for the proteoglycan assay. Once the aliquot was taken from the sample, the deionized water was removed from the vial and replaced with fresh deionized water so that the perfect sink assumptions can be made for the mathematical modeling for the solute release. The samples were taken until no more glucosamine sulfate could be detected in the aliquot sample.

2.7.3 Colorimetric Determination of Glucosamine Sulfate

To observe if the DMMB dye would detect the presence of glucosamine sulfate at higher concentrations, the casted film containing glucosamine sulfate was coated with 1 mL of DMMB so that the surface of the film would be coated. The excess dye was removed and water was added to the weigh boat. The water was removed every hour in order to observe if the staining would decrease as glucosamine sulfate was released. The films containing sodium cellulose sulfate was used as a control.

2.8 Comparison of Mathematical Models

To compare the power law model and the diffusional release in cylindrical coordinates, the release data from the three cases were fitted to the power law and the diffusional release in cylindrical coordinates equation with the mutual diffusional coefficient being unknown. The manipulation of the equations were done in Matlab. The coding is given in Appendix A.

CHAPTER 3

RESULTS AND DISCUSSION

3.1 Swell Test

The increase in fiber diameter of the electrospun gelatin fibers infused with glucosamine sulfate were evaluated by swelling the fibers over a short period time since the water inclusion into the fibers rapidly occurs, which would lead to rapid release of the solute. Through the process used for the swell test, there were inconsistencies with the weights of the swollen fibers since the fibers were allowed to partially dry in order to remove the excess water that was not trapped within the fibers. Table 3.1 contains the calculated swell ratio after averaging the weights of the swollen fibers over the span of the tests.

Table 3.1: Swell Ratio of Gelatin Fibers Infused with Glucosamine Sulfate

Weight Percent Crosslinker in solution (wt% in fibers)	**Initial Weight** g	**Average Swollen Weight** g	**Standard Deviation** g	**Swell Ratio** %
3 wt% (9.40-9.76 wt %)	0.0015g	0.0126g	0.0028g	740%
5 wt% (14.25-15.80 wt%)	0.0044g	0.0521g	0.0117g	1084%
7 wt% (18.90-19.65 wt%)	0.0059g	0.0603g	0.0139g	922%

The fibers swelled as expected. However, the swell ratio of the gelatin fibers that contained more weight percent crosslinker were expected to be lower than the gelatin fibers that contained less weight percent of the crosslinker. The deviation from the expected trend may be caused by the fact that IBO may have not been evenly distributed

in solution prior to electrospinning or that the fibers were not fully heat treated to allow for further crosslinking to occur.

3.2 Measurements of Electrospun Fibers

The electrospun fibers for each case were successfully viewed with the SEM. Measurements of the fiber diameters were obtained since the diffusional release from cylindrical coordinates is dependent on the radius of the fibers. The measurements for the gelatin fibers infused with glucosamine sulfate were not taken since the fibers ended up forming a film after being allowed to swell for 12 hours.

Table 3.2: Average Fiber Diameters of Electrospun Fibers

Fiber Type	**Average Fiber Diameter** nm	**Standard Deviation** nm
Chitosan Fibers Infused with PFTBA	232.32 nm	98.40 nm
Gelatin Fibers Infused with Glucosamine Sulfate	----------	----------
Gelatin Fibers Infused with Sodium Cellulose Sulfate	7000 nm	Not Given

3.3 Release Studies

3.3.1 Oxygen Release from Chitosan Fibers Infused with PFTBA

The chitosan fiber infused with PFTBA mat used for the experiment weighed 0.1326g. The initial dissolved oxygen in the deoxygenated water was 0.600 mg/L. When the mat was added to the water, the dissolved oxygen concentration increased by 0.425 mg/L to reach a value of 1.02 mg/L. Figure 3.1 displays the release profile of the oxygen from PFTBA into the deoxygenated water. The initial dissolved oxygen concentration has been

subtracted from the readings and the readings were divided by the final dissolved oxygen concentration since it was assumed that all of the oxygen would release from PFTBA because the attraction of oxygen to water would be stronger than the van der Waals bonds that hold oxygen to the PFTBA structure.

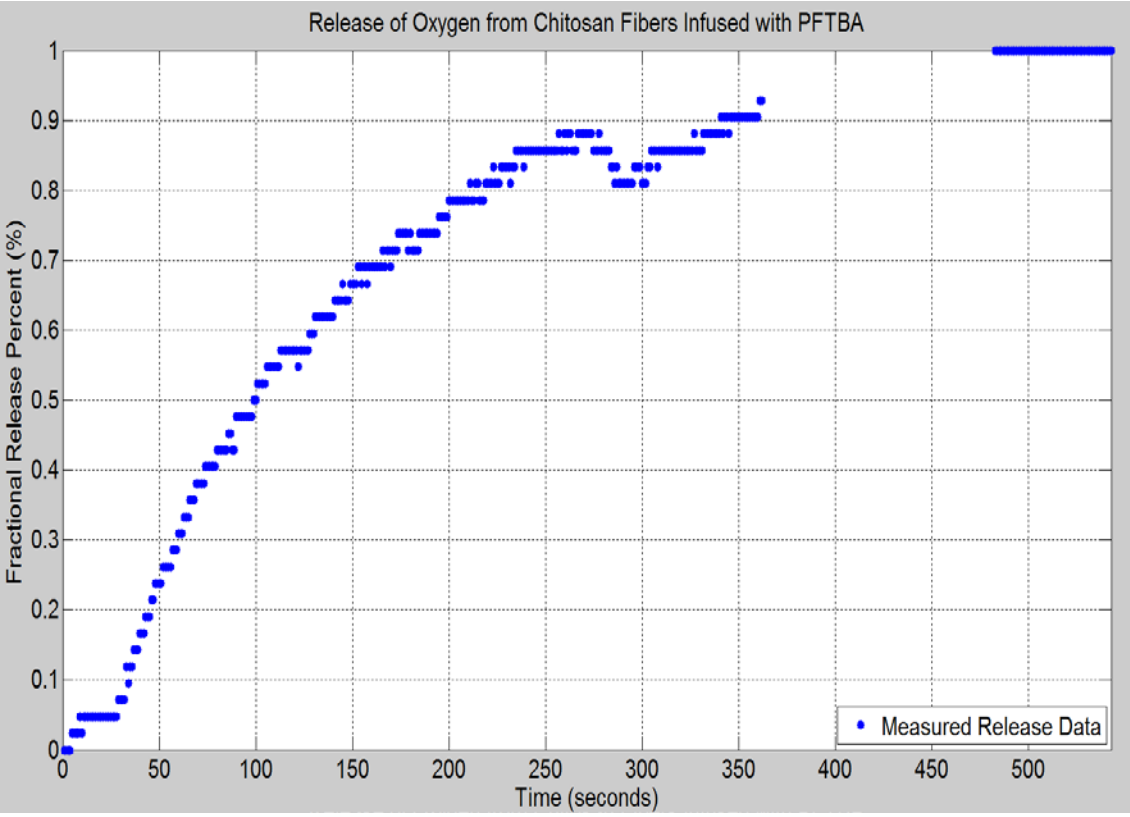

Figure 3.1 Release of oxygen from chitosan fibers infused with PFTBA.

The dissolved oxygen in the water gradually increased as time passed. However, there is a decrease in the curve at around 275 seconds. The decrease in the dissolved oxygen in water may be caused by the stirring required to take the oxygen measurements with the oxygen probe. The disruption in the oxygen measurements from stirring is evident when the oxygen release is plotted as connected points. The gap in measurements between approximately 375 seconds to 475 seconds was caused by the lack of continuous

readings. The oxygen probe can only collect 180 seconds of data at a time before another data collection can begin, so there were some discontinuances in the readings.

3.3.2 Proteoglycan Assay and Colorimetric Determination Results

The DMMB dye was tested by making a standard curve with known concentrations of glucosamine sulfate in deionized water before conducting the release studies with the fabricated gelatin fibers infused with glucosamine sulfate. The created DMMB dye did not change colors when the dye was added to the standard solutions in an one to one ratio of dye to the standard. Additionally, the dye did not react when the dye concentration was doubled by adding twice the amount of dye into the dye solution.

In order to see if the DMMB dye solution was formulated properly, a solution of 10μg/mL sodium cellulose sulfate in deionized water was created. The DMMB dye was tested in an aluminum weight boat by adding 1 ml of the sodium cellulose sulfate solution to 1 ml of the dye. The DMMB dye changed from the initial dark blue color to a bright pink color upon contact with the sodium cellulose sulfate solution. Additionally, the higher concentration DMMB dye reacted with the sodium cellulose sulfate by changing from dark blue to a bright pink color. However, the higher concentration DMMB dye was less stable than the prepared dye and most of the dye precipitated out from solution.

Films with either sodium cellulose sulfate or glucosamine sulfate were fabricated in order to determine if the films could be stained in order to determine to release from the films. The amount of the additive in the film would be determined by the color of the film. Both films should have about the same color intensity since both films have the

same wt% of the additive. However, only the films containing sodium cellulose sulfate turned pink when the films were coated with the DMMB dye. The lack of color change in the film containing glucosamine sulfate suggests that either the concentration of glucosamine sulfate was too low for the DMMB dye to detect or that the dye would not interact with the monosaccharide structures of glycosaminoglycans.

Since the DMMB dye did not react with glucosamine sulfate, other methods of detecting sulfate were pursued. Initially, indirect atomic absorption spectroscopy was considered since sulfate can be measured indirectly by reacting sulfated samples with a barium chloride. However, the method was not practical for the study since the samples would have to be treated overnight and the samples had to be on the order of 10 ml per sample in order for the method to work. Other methods that were considered includes UV/vis spectroscopy and FTIR spectroscopy. In the end, both methods were turned down since the level of glucosamine sulfate in the samples that would be taken as the glucosamine sulfate diffused from the gelatin scaffolds would be in the order of ppm and the noise from the presence sulfur groups in gelatin would make the detection of sulfate unreliable. In addition, the absorbance of UV by glucosamine sulfate would occur in the lower end of the spectrum (100-200 nm range) where the absorbance by glucosamine sulfate would be mixed with the UV absorbance of any other material present in the sample. The only way to get a close measurement of the sulfate present in the release samples would be to send the samples out for sulfur analysis. Thus, the release study for glucosamine sulfate from the electrospun fibers was not conducted since the glucosamine sulfate release was too low to detect and the sulfur analysis would not be practical since multiple samples would have to be sent out.

3.4 Mathematical Model Fitting to Release Data

3.4.1 Overview of Calculations

Both the power law and the diffusional release from cylindrical coordinates equation were used to model the release for both oxygen release from chitosan fibers infused with PFTBA and sodium cellulose sulfate release from gelatin fibers infused with sodium cellulose sulfate. The release data were either measured or given for the study. However, the diffusional release from cylindrical coordinates equation requires a known mutual diffusion coefficient in order to predict fractional release of a solute. Thus, the power law was fitted to the release data. Since the diameter of the fibers were known, the relationship between the power law and the diffusional release from cylindrical coordinates was used to find the mutual diffusion coefficient for the solute in the electrospun fibers.

Once the mutual diffusion coefficient was calculated, the mutual diffusion coefficient and the radius of the fibers were used in the diffusional release from cylinder coordinates equation to solve for the fractional release of the solute. The fractional release of the solute predicted by the calculated mutual diffusion coefficient over predicted the release so the mutual diffusion coefficient was adjusted manually until the fractional release from the calculated mutual diffusion coefficient was similar to the power law prediction. By having a lower adjustment factor, the plot would be less steep as the plot levels off at a lower fractional release value when compared to the release based on the unadjusted mutual diffusion coefficient. When the adjust factor is higher, the plot would become steeper as the plot levels off at a higher fractional release value

when compared to the release based on the unadjusted mutual diffusion coefficient. Thus, the estimate that k can be the equivalent of the first term of the expanded diffusional release from cylindrical coordinates equation (equation 1.8) may not hold true for solving the mutual diffusion coefficient.

To account for the adjustment factor that was used to get the fractional release calculated with the calculated mutual diffusion coefficient within range of the experimental release, the first three terms from the expanded diffusional release from cylindrical coordinates equation (equation 1.7) were used to solve for the mutual diffusion coefficient. In order to solve for the mutual diffusion coefficient, the first three terms of equation 1.6 were considered. The release data was non-linearly fitted by the following model (equation 3.1).

$$\frac{M_t}{M_\infty} = At^{1/2} - Bt - Ct^{3/2} \tag{3.1}$$

With the nonlinear fit of the release data, the coefficients, A, B, and C, could be used to solve for the mutual diffusion coefficient of each term of the expansion (equation 1.7).

$$A = 4\left(\frac{D_{12}}{\pi a^2}\right)^{1/2} \tag{3.2}$$

$$B = \pi\left[\frac{D_{12}}{\pi a^2}\right] \tag{3.3}$$

$$C = \frac{\pi}{3}\left[\frac{D_{12}}{\pi a^2}\right]^{3/2} \tag{3.4}$$

By setting A, B, and C to the corresponding expansion terms, the mutual diffusion coefficient can be solved for each expansion term.

$$D_{12} = \frac{A^2 * a^2 * \pi}{16} \tag{3.5}$$

$$D_{12} = Ba^2 \tag{3.6}$$

$$D_{12} = \frac{C^{2/3} * \pi * a^2}{(\frac{\pi}{3})^{2/3}} \tag{3.7}$$

By solving for the mutual diffusion coefficient based on each coefficient, the calculated mutual diffusion coefficients should become roughly the same value. However, the calculated mutual diffusion coefficient terms were not calculated to be roughly the same value. Additionally, either the second or third calculated mutual diffusion coefficient resulted in a negative mutual diffusion coefficient depending on the value of the B and C coefficient terms found through the nonlinear fit. Thus, only the positive calculated mutual diffusion coefficients were considered and the calculated mutual diffusion coefficients were used to calculate a predicted release profile. In both cases, only the calculated mutual diffusion coefficient produced by the first term of the expansion resulted in a predictive release profile that was similar to the release data, but the predictive release profile either overestimated or underestimated the amount of release. The expanded diffusional release from cylindrical coordinates may not be able to represent the release data for the studied release cases.

In most cases, the predicted fractional solute release for the two release cases could not be predicted accurately with the calculated mutual diffusion coefficient based on the relationship between the power law and the diffusional release from cylindrical coordinates. To figure out of the discrepancy was caused by the fact that the fibers in both cases were swelling as the solute was releasing, a mutual diffusion coefficient was chosen and the radius of the fiber was set to vary throughout the release. Lastly, the release for the initial radius and the swollen release were calculated in order to better understand the effect of swelling on the fraction of solute release.

3.4.2 Model Fitting to Oxygen Release Data

The oxygen release data used for model fitting is the same data collected from the release study and presented in section 3.3.1. After obtaining the data, the data was plotted in Matlab so Matlab's the curve fitting application could be used to obtain the power law. From the curve fitting application, the data was fitted by the following equation.

$$\frac{M_t}{M_\infty} = 0.529t^{0.2054} - 0.8552 \tag{3.8}$$

where

k is equal to 0.529.

n is equal to 0.2054.

R^2 of the fitting was equal to 0.9565.

There is an additional subtraction term included in the fitted power law equation since the release includes a small segment where the oxygen still has not released from the mat.

The value of the term is negative to shift the power law plot to the right so that the power law could better fit the data. The plot of the power law equation and the experimental data is given in figure 3.2.

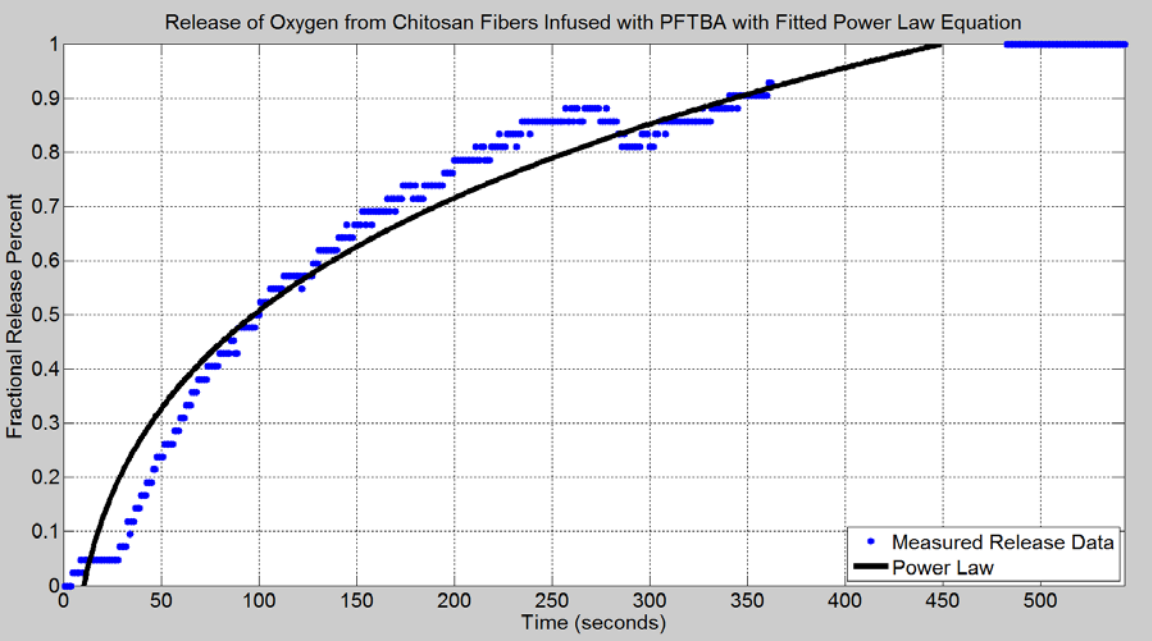

Figure 3.2 Release of oxygen from chitosan fibers infused with PFTBA with fitted power law equation.

The power law is plotted as a black solid line while the release data is plotted as blue points. The power law does follow the increasing trend in the experimental data. However, the noise present in the oxygen reading prevents the power law from being a better fit to the experimental data. If the noise was filtered out from the experimental data, the power law would be a better fit. However, filtering out the noise may remove important features of the release profile.

The mutual diffusion coefficient of oxygen in the chitosan mat was predict based on equation 1.7. Though chitosan fibers are known to swell in an aqueous environment, the measurements of the swollen fiber diameter were not taken. Thus, the chitosan fibers

are assumed to have a constant radius, where the average fiber diameter is 232.32 nm. The calculated mutual diffusion coefficient based on the relationship of the power law to the diffusional release from cylindrical coordinates was $7.414*10^{-16}$ m^2/s. The calculated mutual diffusion coefficient was used to solve for the fraction release percent and was plotted against the power law fit, as shown in figure 3.3.

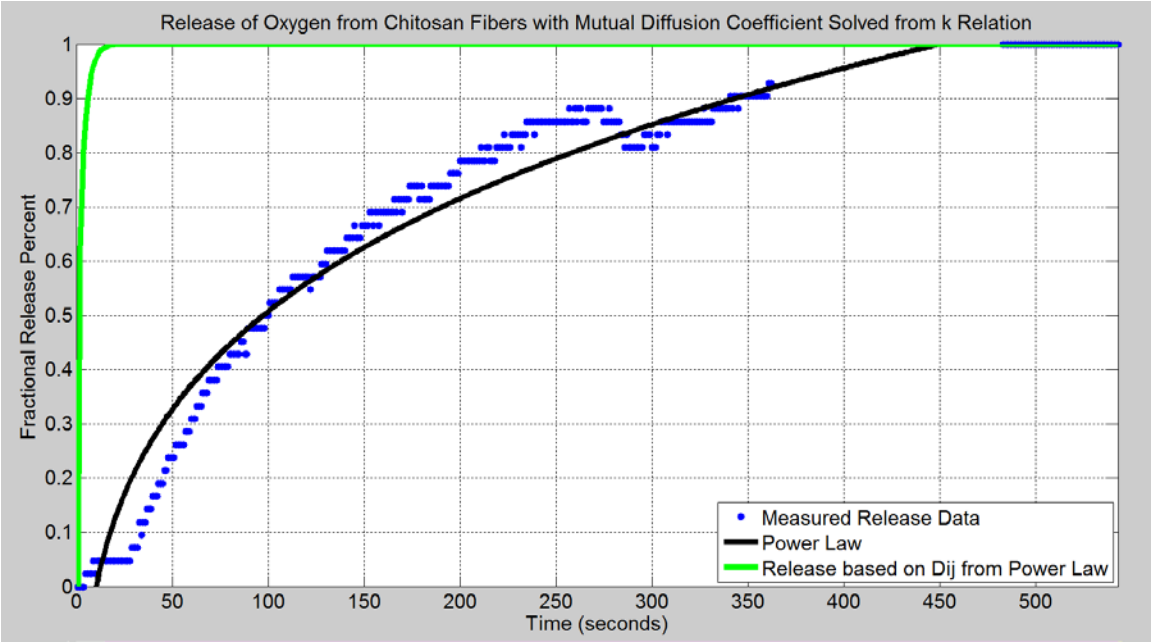

Figure 3.3 Comparison of release models for oxygen from chitosan fibers with mutual diffusion coefficient solved from k relation.

In addition to the previously plotted data, the calculated mutual diffusion coefficient based on the power law is shown in green. Based on the plot, the calculated diffusion coefficient based on the power law relationship to the diffusional release from cylindrical coordinates equation over predicts the release. The calculated mutual diffusion coefficient was multiplied by an adjustment factor of 0.022 in order to make the mutual diffusion coefficient equal to $1.6311*10^{-17}$ m^2/s. The adjusted mutual diffusion

coefficient was used to solve for the fractional release percent and was plotted below in figure 3.4.

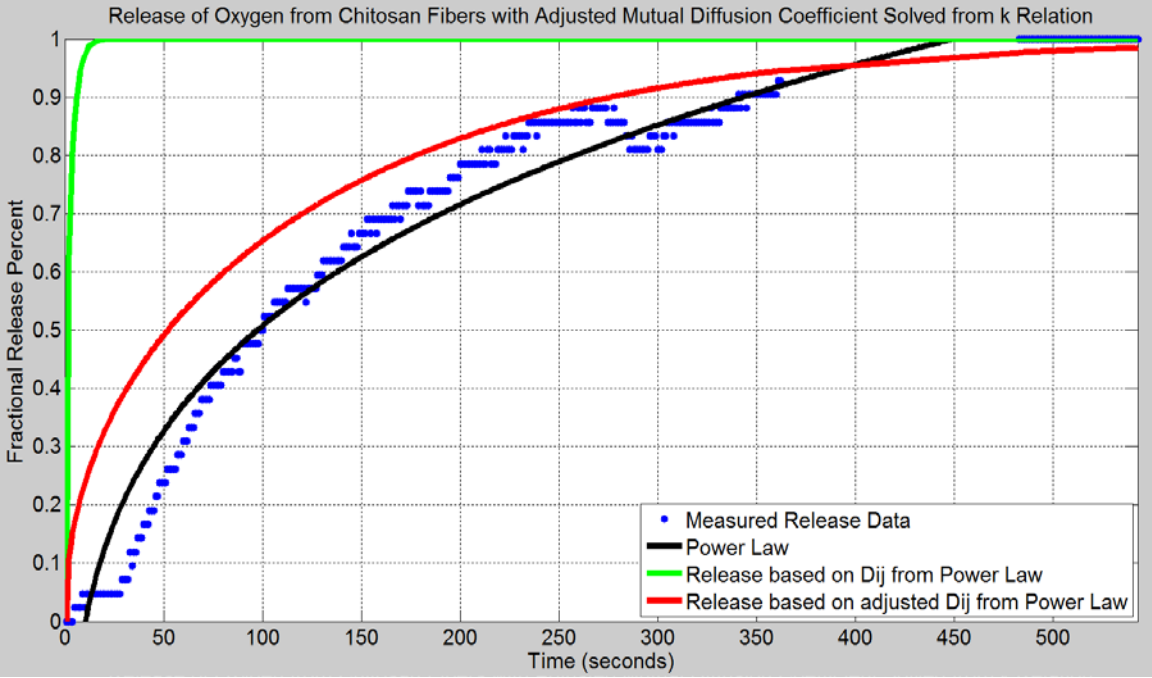

Figure 3.4 Comparison of release models for oxygen from chitosan fibers with adjusted mutual diffusion coefficient solved from k relation. Note: the adjustment value was 0.022.

In addition to the previously plotted data, the release based on the adjusted mutual diffusion coefficient is plotted in red. By decreasing the mutual diffusion coefficient, the maximum release percentage decreased and the slope of the release profile became less steep. In addition, the release profile became closer to the power law release profile.

As stated in section 3.4.1, the first three terms of the expanded diffusional release from cylindrical coordinates equation set equal to the nonlinear fit (equation 3.1) of the release data. The nonlinear fit has an R^2 value of 0.9579. The fit is shown in equation 3.9 below.

$$\frac{M_t}{M_\infty} = (0.03335)t^{1/2} - (-0.001404)t - (7.218 * 10^{-9})t^{3/2} \quad (3.9)$$

From the using equations 3.5, 3.6, and 3.7, the mutual diffusion coefficients were solved based on the coefficients of equation 3.9. The second term produced a negative mutual diffusion coefficient term, so the mutual diffusion coefficient was excluded from the study. Based on the first and third term, the mutual diffusion coefficients were found to be $2.9467*10^{-18}$ m^2/s and $1.5353*10^{-19}$ m^2/s respectively.

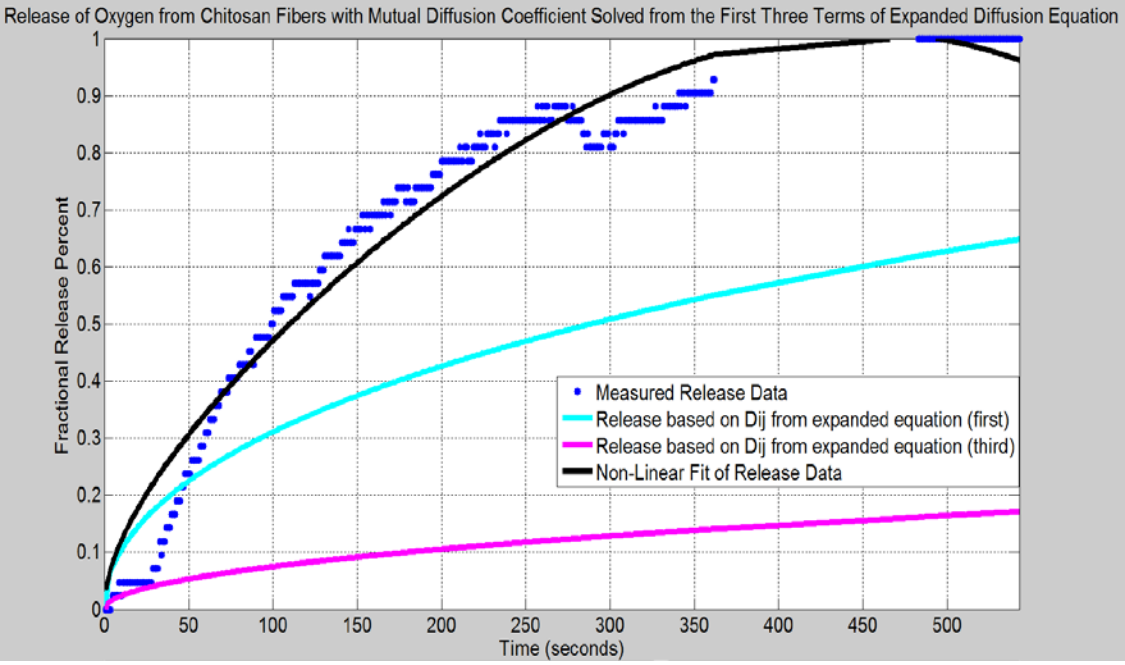

Figure 3.5 Release of oxygen from chitosan fibers with mutual diffusion coefficient solved from the nonlinear fit and the first three terms of expanded diffusion equation.

The measured data is represented by blue dots while the release based on the calculated mutual diffusion coefficient from the first term is represented by the cyan/light blue line and the release based on the calculated mutual coefficient from the third term is represented by the magenta line. The nonlinear fit is represented by the black line. The release profile from the calculated mutual diffusion coefficient from the first term of the

expanded equation provided the closest fit between the two calculated mutual diffusion coefficients. However, both calculated mutual diffusion coefficients produce predictive release profiles that underestimate the rate of release. Thus, the mutual diffusion coefficients produced by the relationship between the expansion of the diffusional release from cylindrical coordinates and the nonlinear fit do not represent the mutual diffusion coefficient of oxygen from the chitosan fibers.

As a comparison of the calculated mutual diffusion coefficients, the plots of the release profiles based on the calculated mutual diffusion coefficients is given in figure 3.6. From the figure, the power law seems to be the best fit. The adjusted mutual coefficient based on relationship between the power law seems to be the second best fit release profile since the relation tends to overestimate the release data by a smaller error in comparison to the other profiles. The large differences in the release profiles between the calculated mutual diffusion coefficients may be caused by the fact that the mutual diffusion coefficient cannot be easily estimated by the mathematical equations utilized in the study. However, the noise within the oxygen release data may also be attributed to the poor model fittings. The release study of oxygen from the chitosan fibers infused with PFTBA should be conducted over again so that the data is reproducible before another attempt on calculating the mutual diffusion coefficient is made.

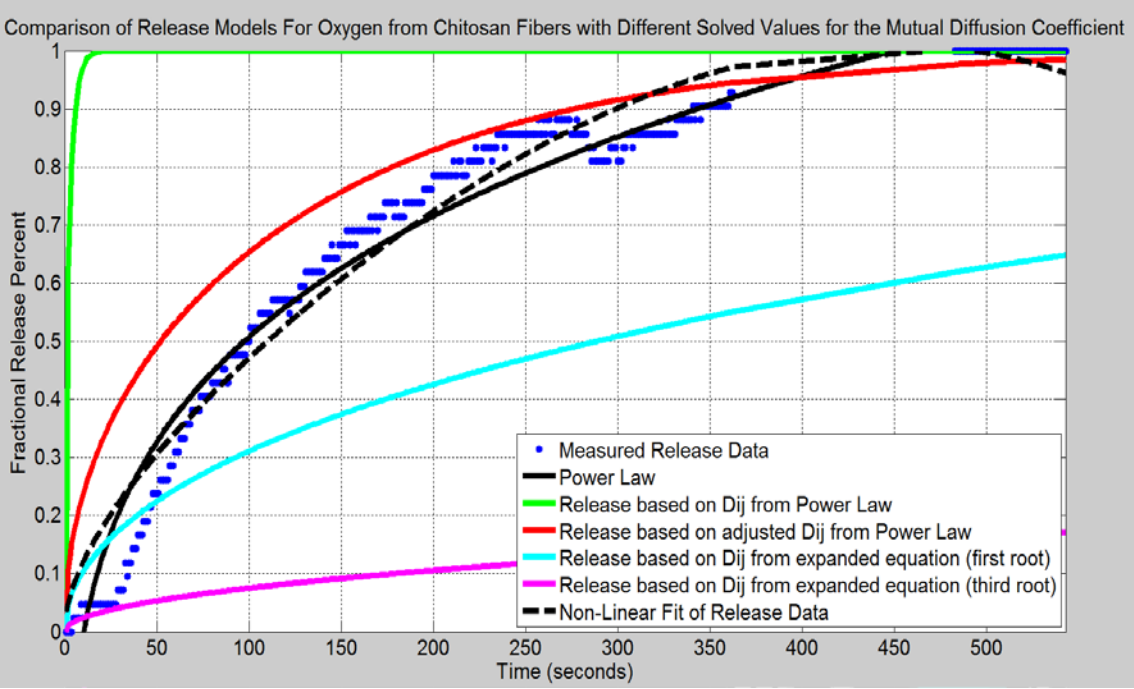

Figure 3.6 Comparison of release models for oxygen from chitosan fibers with different solved values for mutual diffusion coefficient.

3.4.3 Model Fitting to Sodium Cellulose Sulfate Release Data

The release data for sodium cellulose sulfate from gelatin infused with sodium cellulose sulfate was obtained from Gloria Portacerreo. In Portacerreo's study, she took six samples from her electrospun gelatin fibers containing 5 wt% sodium cellulose sulfate and conducted her release study over the course of 42 days. About 14% of the total sodium cellulose sulfate was release from the samples. For this study, the average of the six releases were taken as the release data. Figure 3.8 is a plot of the average release of sodium cellulose sulfate over the course of 42 days.

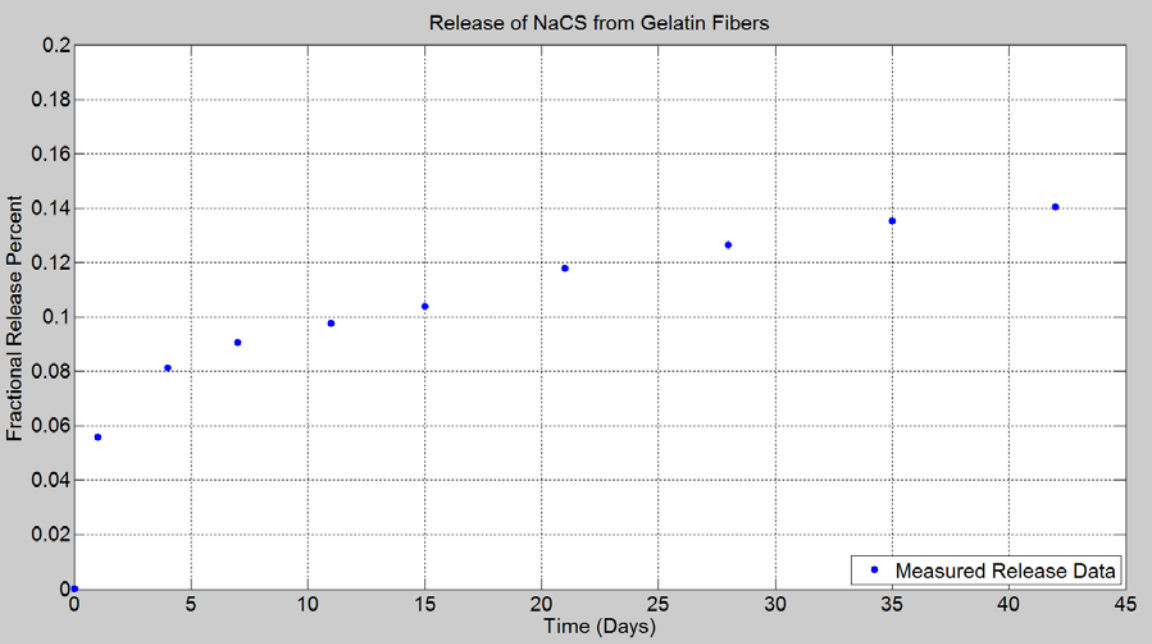

Figure 3.7 Release of sodium cellulose sulfate (NaCS) from gelatin fibers.

The release data is represented by the blue points on the graph. Matlab's curve fitting application was used to fit the release data to the power law equation. The following equation was obtained from the fitted equation.

$$\frac{M_t}{M_\infty} = 0.05553t^{0.2466} \tag{3.10}$$

where

k is equal to 0.05553.

n is equal to 0.2466.

R^2 of the fitting was equal to 0.9974.

From the obtained power law equation, the power law could be plotted against the release data, which is shown in figure 3.8.

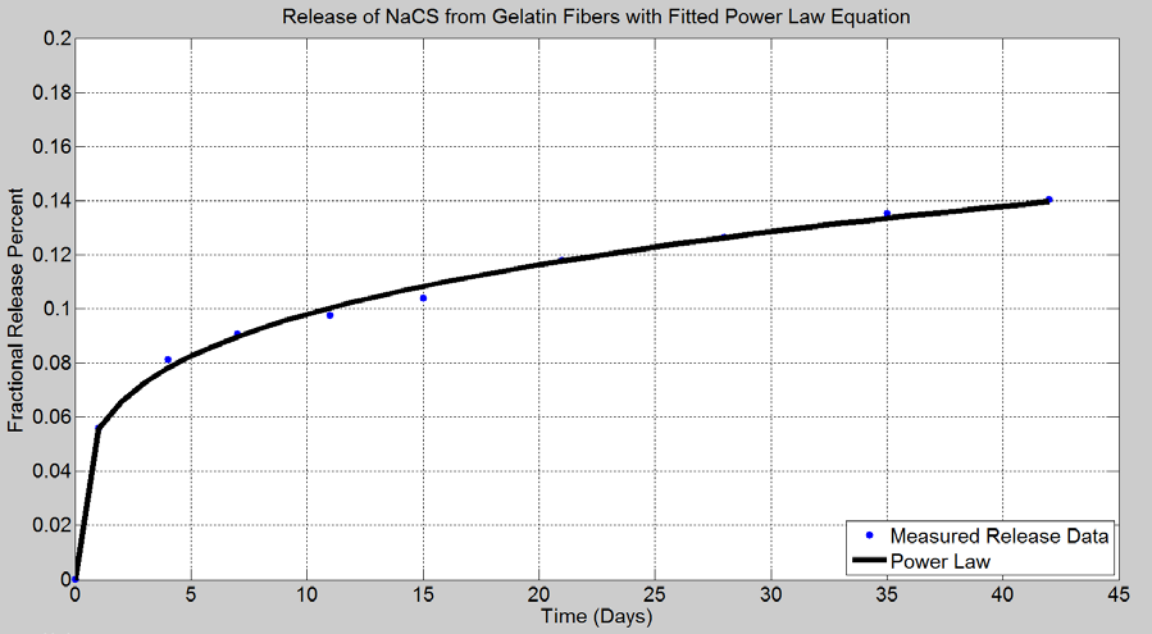

Figure 3.8 Release of NaCS from gelatin fibers with Fitted Power Law Equation.

In addition to the previously plotted data, the power law is plotted as a black line. Based on the plot and the R^2 value, the power law seems to fit the release data well. Additionally, there is little to no noise in the release data in comparison to the release data of oxygen from chitosan fibers infused with PFTBA. Thus, noise should not be a large factor during the data analysis.

In order to calculate the mutual diffusion coefficient, the average diameter of the gelatin fibers was given to be 7 μm. Gelatin fibers are known to swell in an aqueous fiber, but only one fiber diameter was given. Since only one fiber diameter was given, the gelatin fibers are assumed to have a constant diameter of 7 μm. Based on the given information, the mutual diffusion coefficient can be solved through the relationship between the power law and the diffusional release from cylindrical coordinates equation (given in equation 1.7). The calculated mutual diffusion coefficient based on the relation between the power law and the diffusional release from cylindrical coordinates was

7.4169*10^{-15} m^2/day. The calculated mutual diffusion coefficient was used to solve for the fraction release percent and was plotted against the power law fit, as shown in figure 3.9.

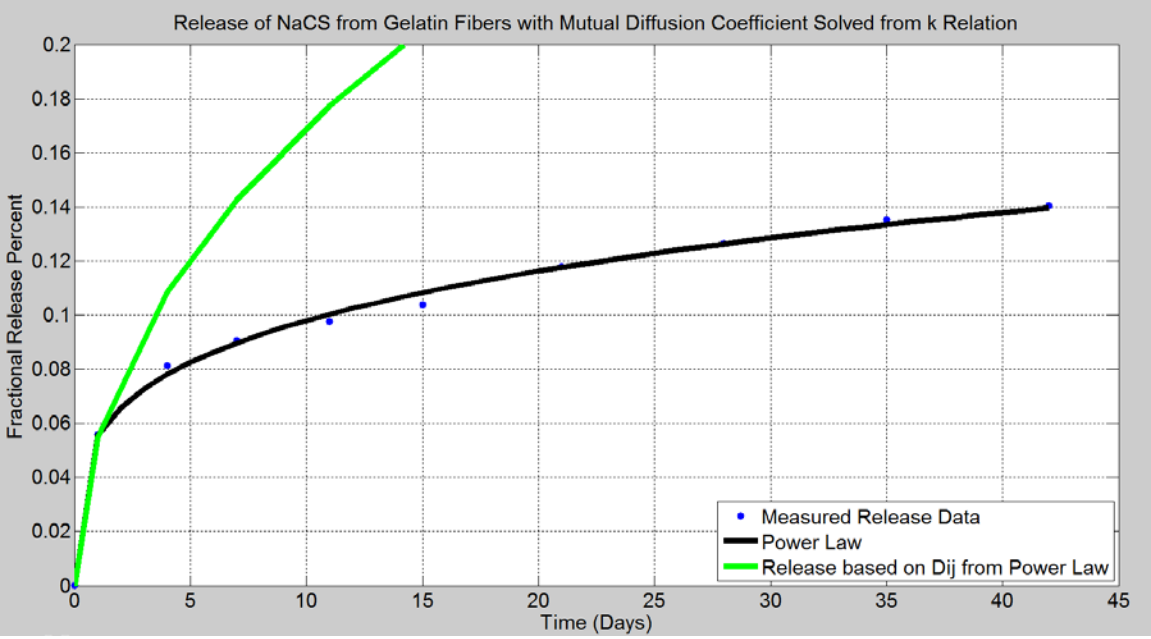

Figure 3.9 Comparison of release models for NaCS from gelatin fibers with mutual diffusion coefficient solved from k relation.

In addition to the previously plotted data, the calculated mutual diffusion coefficient based on the power law is shown in green. Based on the plot, the calculated diffusion coefficient based on the power law relationship to the diffusional release from cylindrical coordinates equation over predicts the release for every day after the first day. The calculated mutual diffusion coefficient was multiplied by an adjustment factor of 0.25 in order to make the mutual diffusion coefficient equal to 1.8542*10^{-15} m^2/day. The adjusted mutual diffusion coefficient was used to solve for the fractional release percent and was plotted below in figure 3.10.

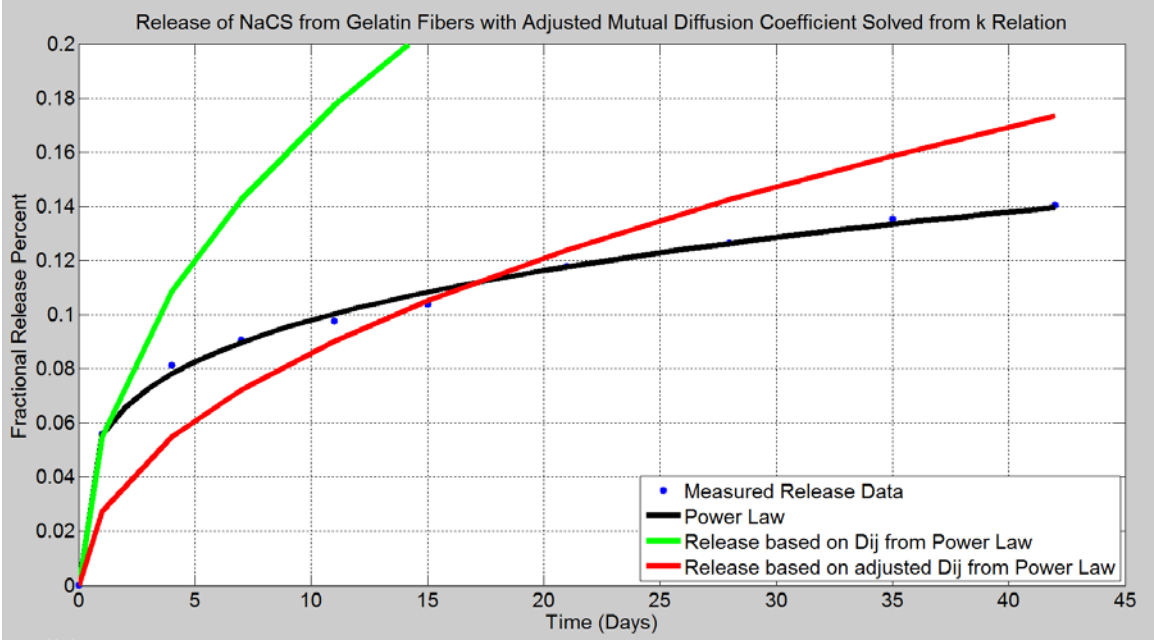

Figure 3.10 Comparison of release models for NaCS from gelatin fibers with adjusted mutual diffusion coefficient solved from k relation Note: adjustment value was 0.25.

In addition to the previously plotted data, the release based on the adjusted mutual diffusion coefficient is plotted in red. By decreasing the mutual diffusion coefficient, the maximum release percentage decreased and the slope of the release profile became less steep. In addition, the release profile became closer to the power law release profile. However, the initial phase for the release profile based on the adjusted mutual diffusion coefficient underestimates the release until day 17 where the release profile starts to over predict the release after day 17.

As stated in section 3.4.1, the first three terms of the expanded diffusional release from cylindrical coordinates equation set equal to the nonlinear fit (equation 3.1) of the release data. The nonlinear fit has an R^2 value of 0.9814. The fit is shown in equation 3.11 below.

$$\frac{M_t}{M_\infty} = (0.05003)t^{1/2} - (0.005727)t - (-1.633 * 10^{-6})t^{3/2} \quad (3.11)$$

From the using equations 3.5, 3.6, and 3.7, the mutual diffusion coefficients were solved based on the coefficients of equation 3.11. The third term produced a negative mutual diffusion coefficient term, so the mutual diffusion coefficient was excluded from the study. Based on the first and second term, the mutual diffusion coefficients were found to be $6.0204*10^{-15}$ m^2/s and $7.0156*10^{-14}$ m^2/s respectively.

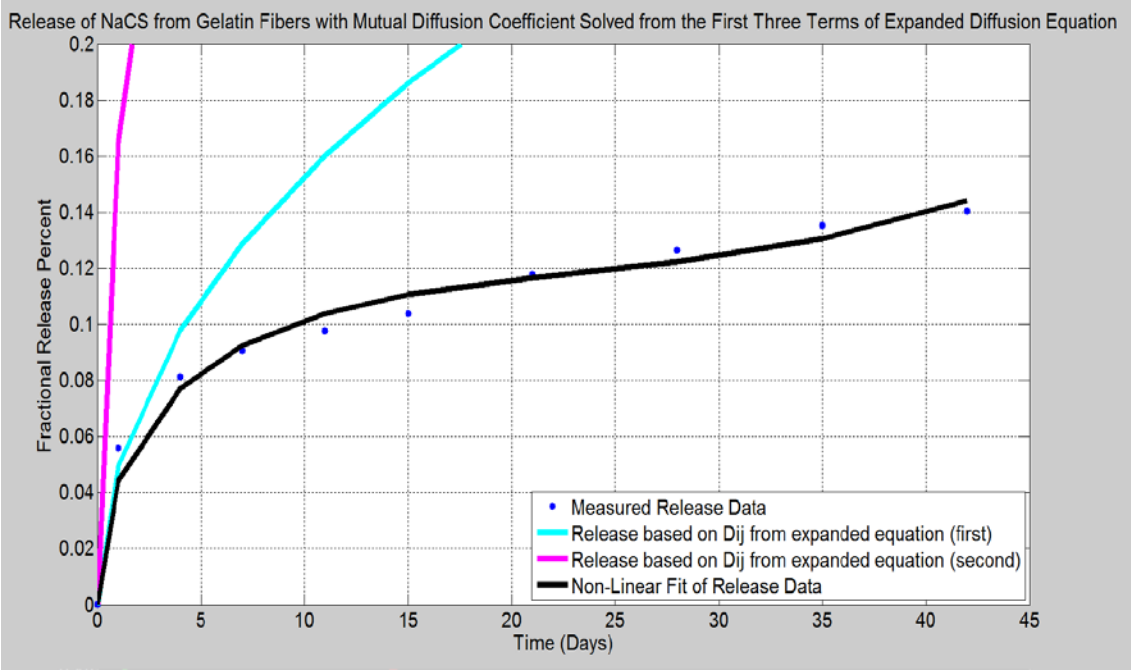

Figure 3.11 Release of NaCS from gelatin fibers with mutual diffusion coefficient solved from the nonlinear fit and the first three terms of expanded diffusion equation.

The measured data is represented by blue dots while the release based on the calculated mutual diffusion coefficient from the first term is represented by the cyan/light blue line and the release based on the calculated mutual coefficient from the second term is represented by the magenta line. The nonlinear fit is represented by the black line. The

release profile from the calculated mutual diffusion coefficient from the first term of the expanded equation provided the closest fit between the two calculated mutual diffusion coefficients. However, both calculated mutual diffusion coefficients produce predictive release profiles that overestimates the rate of release. Thus, the mutual diffusion coefficients produced by the relationship between the expansion of the diffusional release from cylindrical coordinates and the nonlinear fit do not represent the mutual diffusion coefficient of sodium cellulose sulfate from gelatin fibers.

As a comparison of the calculated mutual diffusion coefficients, the plots of the release profiles based on the calculated mutual diffusion coefficients is given in figure 3.12. From the figure, the power law seems to be the best fit. The adjusted mutual coefficient based on relationship between the power law seems to be the second best fit release profile since the relation tends to under and overestimate the release data by a smaller error in comparison to the other profiles. The large differences in the release profiles between the calculated mutual diffusion coefficients may be caused by the fact that the mutual diffusion coefficient cannot be easily estimated by the mathematical equations utilized in the study. Additionally, the models tend to overestimate release of sodium cellulose sulfate while the models used for oxygen release tend to underestimate the release. Besides for the difference in the electrospun fiber polymer, the release differ based on the size of the solute. Thus, the models may be incapable of accounting for the size of the solute when the power law and the diffusional release from cylindrical coordinates are used to solve for the mutual diffusion coefficient.

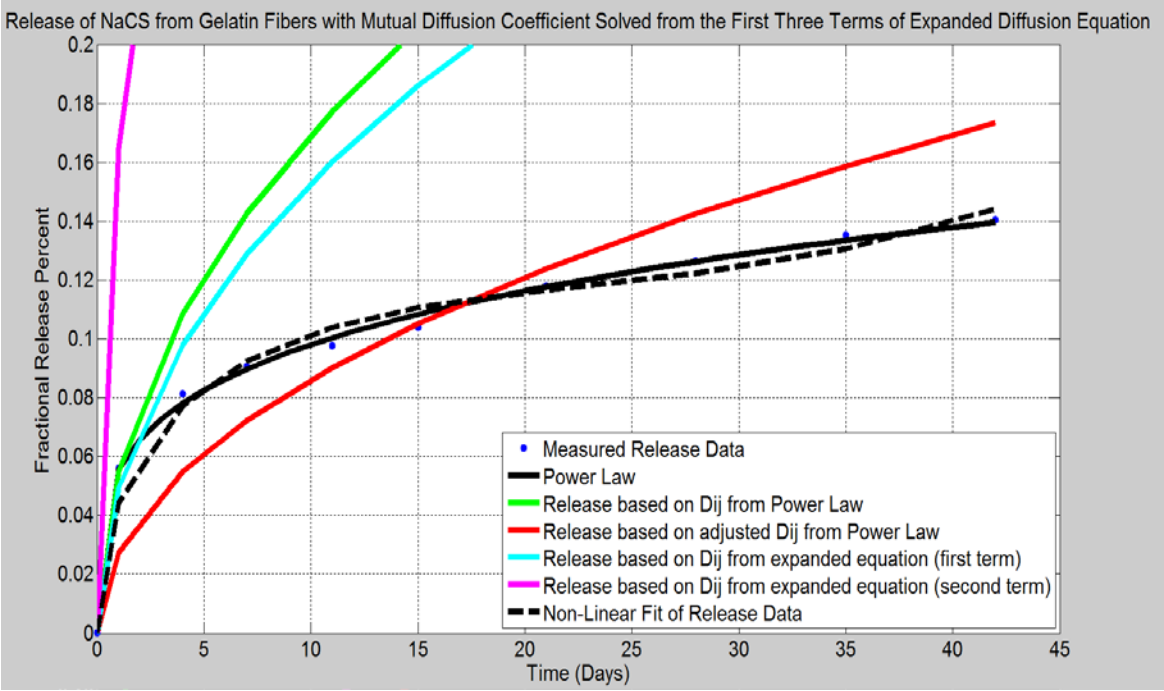

Figure 3.12 Comparison of release models for NaCS from gelatin fibers with different solved values for mutual diffusion coefficient.

3.4.4 Effect of Changing Radius on Release

For both the oxygen release and sodium cellulose sulfate release study, the electrospun fibers are capable of swelling, but the radius of the fibers were assumed to be constant since the initial and swollen diameters were not measured. However, the assumption that the radius is constant for both release studies may be the reason why the diffusional release from cylindrical coordinates could not accurately represent the release data with the calculated mutual diffusion coefficients. In order to better understand the effect of the radius change on the release profile, the radius was set to increase linearly from an initial diameter to a swollen diameter. For this part of the study, the mutual diffusion coefficient was set to be constant value. For figure 3.15 and 3.16, the diffusion coefficient was kept to $9*10^{-16}$ m^2/day. The initial and swollen diameter values were given from Lakshit Tripathi, who measured the diameters of his electrospun gelatin fibers that contained

5wt% and 10wt% crosslinker (IBO) when in solution. Table 3.3 lists the diameters that were given.

Table 3.3: Initial and Swollen Diameters of Gelatin Fibers Containing Different Weight Percent Crosslinker

Weight Percent Crosslinker (IBO) in Solution wt%	**Initial Diameter** m	**Swollen Diameter** m
5wt%	$458*10^{-9}$ m	$2.975*10^{-6}$ m
10wt%	$580*10^{-9}$ m	$1.211*10^{-6}$ m

To compare the effect of the increasing radius, fractional release for when the fiber diameter was the initial diameter, the swollen diameter, and the diameter changing from initial diameter to swollen diameter were plotted. The plots for fibers with 5wt% (figure 3.13) and 10wt% (figure 3.14) are given below.

Figure 3.13 Effect of swelling on release profile from fibers represented by 5wt% crosslinked gelatin fibers. Note: the mutual diffusion coefficient used for the plot was a randomly assigned value of $9*10^{-16}$ m^2/day while the initial and swollen diameters are set to 438 nm and 2.975 μm respectively.

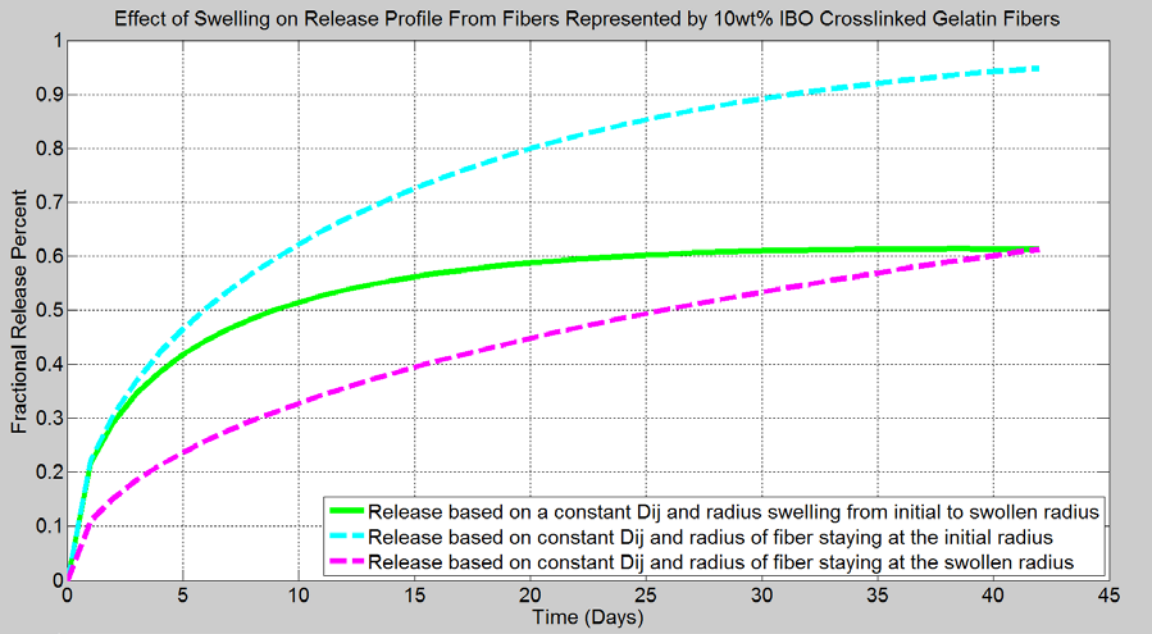

Figure 3.14 Effect of swelling on release profile from fibers represented by 10wt% crosslinked gelatin fibers. Note: the mutual diffusion coefficient used for the plot was a randomly assigned value of $9*10^{-16}$ m^2/day while the initial and swollen diameters are set to 580 nm and 1.211 μm respectively.

In both figures 3.13 and 3.14, the green line represents the release profile with the diameter of the fiber increasing from the initial diameter to swollen diameter. The cyan/light blue dashed line represents the release profile with the diameter of the fiber set to the initial diameter. The magenta dashed line represents the release profile with the diameter of the fiber set to the swollen diameter. By having the radius change from the initial radius to the swollen radius, the resulting release took on the characteristics of the release based on the initial radius while the later part of the release resembled the release based on the swollen radius. Additionally, the fractional release percent decreases during the later part of the release for when the radius increases linearly with time. However, the release data does not have the same feature as the plotted release models. The difference in the release based on a constant mutual diffusion coefficient with the radius of the fiber

increasing to a swollen diameter and the observed release profiles may be accounted for by the relaxation of the polymer chains that occurs during swelling release. During swelling, the characteristics of the solid matrix changes as water enters into the system. Since the characteristics of the matrix is changing, the mutual diffusion coefficient must be changing as the system swells. Thus, the assumption that the mutual diffusion coefficient is constant as the solid matrix swells cannot be used.

3.4.5 Effect of Swelling on Release Studies

In both release studies, the material used are both hydrophilic materials. Thus, the fibers could be considered to be hydrogels, which are hydrophilic crosslinked polymeric networks that are capable of swelling as water enters the system [29]. Since the fibers are hydrogels, the change in radius must be considered when predicting the release profile. In oxygen release study, only the initial fiber diameter was given. If the swollen fiber diameter was obtained, the change in diameter may account for the discrepancies in the release profile. In addition, the mutual diffusion coefficient cannot be assumed to be constant for the reasons stated in section 3.4.4. Thus, the impact of swelling cannot be assumed to be insignificant when considering solute release.

3.5 Account of Difference in Release Data Versus Mathematical Diffusion Model

In this study, the diffusional release from cylindrical coordinates equation was considered as a model for release from the nanofiber scaffolds created through electrospinning. However, the model did not produce a similar release profile when the expanded form of the diffusional release from cylindrical coordinates equation (equation 3.1) was used to

solve for the mutual diffusion coefficient. The following sections are on why the diffusional release from cylindrical coordinates equation did not produce release profiles that were similar to the experimental data.

3.5.1 Quality of the Release Data

The release data should be reproducible since the study had to rely on the release data since the mutual diffusion coefficient of the release systems were unknown. Thus, the calculations of the mutual diffusion coefficient will be affected by the quality of the release data. The importance of having reproducible data is exemplified between the oxygen and sodium cellulose sulfate release study.

For the sodium cellulose sulfate release study, six samples were taken from the electrospun fibers and the release profiles of each sample were recorded. There were slight differences in the fraction of total release from each sample, but the overall release for each sample followed a similar release curve. To account for the slight differences in the fractional release, the release data for the six samples was averaged in order to obtain the release data for this study.

In the oxygen release study, only one set of release data was recorded since only a single sample was used for the release study. The entire electrospun chitosan mat infused with PFTBA was used during the release study since the amount of oxygen release from a segment of the mat may not provide a significant enough oxygen release that could be detected by the oxygen probe. Additionally, the oxygen probe only collects information for runs that are less than 180 seconds (3 minutes). There may have been a time delay that was not accounted for when plotting the data. Also, the amount of oxygen loaded in

the mat is unknown since the loading capacity of oxygen by PFTBA within the chitosan fibers is not well understood. Thus, the researcher had to assume that the total amount of oxygen in the mat was release and that data represented the oxygen release from the chitosan fibers infused with PFTBA despite the fact that there are known issues with the data collection.

3.5.2 Experimental Set Up Versus Initial Conditions

For both release systems, the release is assumed to have perfect sink conditions and that the solute is evenly distributed throughout the length of the fiber. If the release study was not conducted to have the same initial and boundary conditions as the equation, the equation will not produce valid results. The solute is assumed to be uniformly distributed in the oxygen and sodium cellulose sulfate release studies. In order to account for the perfect sink case, the media that the solute diffuses into has to be changed at certain intervals. For the sodium cellulose sulfate release, the release medium was changed at regular intervals. For the oxygen release, the deoxygenated water was not changed throughout the release. The release rate would decrease if a perfect sink is not maintained since the difference in concentration between the electrospun fibers and the aqueous environment would have a smaller change. The smaller difference in concentration would decrease the driving force since the diffusion of the solute is causing the solute concentration to reach equilibrium with the inside and outside of the electrospun fibers. Thus, the oxygen concentration within the chitosan fibers infused with PFTBA may be greater than what was released and the assumption that the total amount of oxygen loaded into the fibers were released may not be correct.

In addition to the initial and boundary conditions, the experimental set up does not model the same release as the diffusional release from cylindrical coordinates equation. Either segments of the electrospun fibers were taken from the electrospun mat or the whole electrospun fiber mats were used for the release studies. Therefore, the release measurements are not from a single thread as assumed by the diffusional release from cylindrical coordinates equation. Instead, the mat consists of multiple cylinders of various sizes and lengths depending on the parameters used to electrospin the fibers. Additionally, the fibers within the mat do not have to run parallel with each other nor have the same radius. In most cases, the electrospun fibers are not uniformly arranged since the fibers formed through electrospinning are unwoven. Thus, the diffusional release from cylinders may be an inappropriate model for representing the release from nanofibers unless if a single thread is sampled from the mat.

3.5.3 Comparison of Model Geometry

Other geometry should be considered since the diffusional release from cylindrical coordinates equation could not represent the release data. The release could be considered from a line source, thin film, or a slab since the diameters of the fibers are small in respect to the dimensions of the samples and the distance that the solute has to travel in order to reach the release medium. Additionally, the fibers could be considered as a porous structure where the distance between fibers are considered to be the pores and the fibers are considered as the solid phases.

CHAPTER 4

CONCLUSIONS

The objective of this study was the evaluate the mathematical models that are used for estimating released based the release for nanofiber scaffolds. Estimates of the mutual diffusion coefficient were obtained by fitting the power law and diffusion release from cylindrical coordinates equations to release studies from electrospun fibers. Additionally, the effect of swelling on the release profile was determined based on initial and swollen diameters from electrospun crosslinked gelatin fibers .

Both chitosan fibers infused with PFTBA and crosslinked gelatin fibers infused with glucosamine sulfate were successfully fabricated through electrospinning. Additionally, gelatin films containing either glucosamine sulfate and sodium cellulose sulfate were created. The swell test of the crosslinked gelatin fibers was successfully conducted.

The release of oxygen from the chitosan fibers infused with PFTBA was successfully measured. However, the release of glucosamine sulfate could not be measured at the level of release that would occur with the fabricated gelatin fibers.

Despite the fact that the release of glucosamine sulfate could not be measured from the electrospun scaffolds, several conclusions can be made from the study of the release of glucosamine sulfate from crosslinked gelatin fibers. 1) A more efficient way of introducing IBO into the solution used to fabricate gelatin fibers infused with glucosamine sulfate is required to fully crosslink the fibers and to prevent the fibers from swelling to the extent seen in the study. Additionally, longer heat treatment times or more IBO may be required to increase the crosslinking. 2) The fibers require a higher weight

percent of glucosamine sulfate in order to detect its release. Detecting the presence of glucosamine sulfate became almost impossible by having the weight percentages of glucosamine sulfate mimicking the biological levels of the substance. The only way to detect the amount of glucosamine sulfate present as it releases from the fibers is the conduct a sulfur elemental analysis, which was not feasible for the study. 3) Dyes used for measuring the concentration of proteoglycans are not sensitive enough to bind to the monosaccharide structure. DMMB did not change color when in the presence of a known concentration of glucosamine sulfate. However, DMMB did change from blue to pink when in the presence of sodium cellulose sulfate in a stock solution made to be the same as the glucosamine sulfate solution. Gelatin films containing either glucosamine sulfate or sodium cellulose sulfate were casted in an attempt to see if increasing the weight percent of glucosamine sulfate would allow the DMMB dye to react with the glucosamine sulfate. Despite the increase in the weight percent of glucosamine sulfate, DMMB did not react to the presence of glucosamine sulfate. The lack of reactivity from DMMB may be caused by the difference in charge strength present between the monosaccharide and glycosaminoglycan structure. In the glycosaminoglycan structure, there are multiple sulfated side groups versus the monosaccharide that has one sulfated side group.

Despite the lack of release data from the intended release study of glucosamine sulfate, the release data from the chitosan fibers infused with PFTBA was usable. Additionally, release data of sodium cellulose sulfate from gelatin fibers was obtain from Gloria Portacerreo. After obtaining the release data and the fiber diameters from the two release studies, a rough estimate of the mutual diffusion coefficient was calculated for

both release studies through the manipulation of the expanded diffusional release from cylindrical coordinates equation. The release profiles calculated with the mutual diffusion coefficient based on the expanded diffusional release from cylindrical coordinate equation underestimated the release profile for the oxygen release study. However, the release profile calculated based on the expanded diffusional release from cylindrical coordinates equation overestimated the release profile for the sodium cellulose release study. The difference in over estimating and underestimating the release profile may be caused by the difference in the size of the solutes in ease release case.

Based on the results of the model fitting of the release studies, the power law and diffusional release from cylindrical coordinates equation has the potential for predicting the mutual diffusion coefficient when the release data is given. However, swelling must be considered since the increase in fiber diameter will affect the release profile. Additionally, noise in the release data should be avoided since the model fitting will not be as efficient in predicting the mutual diffusion coefficient. Lastly, the release data should resemble the same initial conditions that are used to solve for the equation for diffusional release. To get the best results from the manipulation of the mathematical models presented in the study, the initial and swollen fiber diameters should be obtained along with release data from a single fiber that does not contain noise. Other mathematical models should also be explored if release data from a single fiber cannot be obtained.

CHAPTER 5

FUTURE WORK

Currently, the calculated mutual diffusion coefficients have not been used with other release studies to see how closely the values resemble the true mutual diffusion coefficients. In order to test how well the estimated mutual diffusion coefficient reflects the actual mutual diffusion coefficient, the two release systems would have to be fabricated with different radius sizes so that the mutual diffusion coefficient would stay constant while the release profile would change based on the increase or decrease of solid matrix that the solute has to travel through.

Based on the study, the power law and the diffusional release from cylindrical coordinates equation has the potential for predicting release from electrospun fibers on the nanometer to micrometer scale. However, the power law requires previous release data before creating a predictive mathematical model for future predictions on release for the same release system. If the mutual diffusion coefficient could be predicted without the use of the release data, the diffusional release from cylindrical coordinates equation could be used to predict the release profile of a solute from an electrospun fiber. Other mathematical models should be examined since most measurements are not made with respect to a single fiber. Attempts should be made in predicting or measuring the mutual diffusion coefficient so that the diffusional release from cylindrical coordinates equation can be used as a predictive model for release.

APPENDIX A

MATLAB CODING UTILIZED FOR CALCULATIONS

```
% Note: Coding set for sodium cellulose sulfate release
% Author: Jennifer Moy
% Created: April 18, 2014
% Edited: April 20, 2014
% The purpose of this code is to manipulate the power law
% and diffusional release from cylindrical coordinates
% equation for calculating the mutual diffusion coefficient
% and to create a predictive release profile based on the
% calculated value. The code may be turned into a function
% so that it can be applied to different release data
%% Clear Previous Data
clear all
clc
%% Input Release Data Manually
Release_data=[0.0000000001
0.0559,0.0812,0.0907,0.0976,0.1038,0.1180,0.1265,0.1353,...
     0.1404];
time=[0.0000000001, 1,4,7,11,15,21,28,35,42];
last_data_point=length(Release_data);
count=1;
Release_Data=Release_data;
while count<=last_data_point
    Release_Data(count)=Release_data(count);
    count=count+1;
end
%% Power Law
k=0.05553; % k and n found from curve fitting app in Matlab
n=0.2466; % Curve fitting was done for the
Times=0:1:42;
Length=length(Times);
Power_Law=zeros(1,Length);
Counters=1; %Counter for Power Law Equation
while Counters<=Length
    Power_Law(Counters)=k*Times(Counters)^n;
    Counters=Counters+1;
end
%% Solve for Diffusion coefficient based on first term of
expansion
Ask=input('Do you have an initial and swollen diameter ...
 for your fibers? Y/N ','s'); % To make radius extend over
% a range
```

```
% input used: Ask='N';
if Ask=='Y'
   initial=input('What is the initial diameter of your ...
    fibers before swelling. Give the diameter in meters ');
   swollen=input('What is the swollen diameter of your ...
    fibers after swelling. Give the diameter in meters ');
   initial=initial/2;
   swollen=swollen/2;
else
   d=input('What is the diameter of your fibers. Give ...
    the diameter in meters ');
   % input used d=(7.0*10^-6);
   a=d/2; % Average Radius (given in meters) a=(7.0*10-6)/2
          % meters
end
if Ask=='Y'
    Radius_Increase=(swollen-initial)/(last_data_point-1);
    a=initial:Radius_Increase:swollen;
    Dij_Power_Law=zeros(last_data_point,1);
    for n=1:last_data_point;
        Dij_Power_Law(n)=(((k^2)*pi*((a(n))^2))/16);
    end
else
    Dij_Power_Law=(((k^2)*pi*(a^2))/16);
end
%% Effect of radius
if Ask=='Y'
    Dij_Power_Law_initial=(((k^2)*pi*(initial^2))/16);
    Dij_Power_Law_swollen=(((k^2)*pi*(swollen^2))/16);
end
%% Making adjustments to Diffusion Coefficient to manually
% fit data
adjustment_factor=.25;
Dij_Power_Law_Adjusted=Dij_Power_Law*adjustment_factor;
%% Calculation for Dij based on first three terms of
% expanded series created from the Diffusion from
% Cylindrical Coordinates
Fraction_of_Solute_Release=Release_Data; % Changes for each
% calculation
t=time; % Changes for each calculation
radius=a; % Can either be constant or changing depending on
% input for diameter
Amount_of_Runs=last_data_point;
%% Calculated Dij based on expansion fit
A=0.05003;
B=0.005727;
C=-1.633*10^(-6);
```

```
Expansion_Fit=zeros(time,1);
for n=1:10;
    Expansion_Fit(n)=A*(time(n))^(1/2)-B*time(n)...
     -C*(time(n))^3/2;
end
Dij_first=((A^2)*(a^2)*pi)/16;
Dij_second=(B)*(a^2);
Dij_third=((C^(2/3))*(a^2)*pi)/((pi/3)^(2/3));
%% Enter the calculated Dij into diffusion equation
Time=time; % Time matrix for Dij plotting
Counter=length(time); % counter for the for statement
Release_based_on_Power_Law=zeros(Counter,1);
Release_based_on_Power_Law_Adjusted=zeros(Counter,1);
if Ask=='Y';
    Release_based_on_Power_Law_initial=zeros(Counter,1);
    Release_based_on_Power_Law_swollen=zeros(Counter,1);
end
Release_based_on_first=zeros(Counter,1);
Release_based_on_second=zeros(Counter,1);
x=0:0.001:500;
y=besselj(0,x);
count=length(x); % Upper Limit of bessel j search for zeros
x_zeros=zeros(1,159); % 159=> number of zeros for time
% length x
counter=1; % For bessel j function
Count=1; % Input for zeros
% Bessel J function
while counter<count;
    if y(counter)>0 && y(counter+1)<0;
        x_zeros(Count)=(x(counter)+x(counter+1))/2;
        Count=Count+1;
    elseif y(counter)<0 && y(counter+1)>0;
        x_zeros(Count)=(x(counter)+x(counter+1))/2;
        Count=Count+1;
    else
    end
    counter=counter+1;
end
% Adjusting Bessel J function to reflect Jo(a*alpha) where
% alpha is the roots
if Ask=='Y' % If radius is not constant
    x_zeros_initial=x_zeros/initial;
    x_zeros_swollen=x_zeros/swollen;
    Number_Radius_Inputs=length(a);
    X_Zeros=zeros(Number_Radius_Inputs,159);
    Counts=1; % Counter for inputing Bessel J zeros when
     % radius is not constant
```

```
    while Counts<=Number_Radius_Inputs;
        for n=1:159;
            X_Zeros(Counts,n)=(x_zeros(1,n))/(a(Counts));
        end
        Counts=Counts+1;
    end
    x_zeros=X_Zeros;
else
    x_zeros=x_zeros/a; % If radius is constant
end
% Calculating summation
for n=1:Counter; % Counter=number of time term
    if n==1;
        Release_based_on_Power_Law(Counter)=0;
        Release_based_on_Power_Law_Adjusted(Counter)=0;
        if Ask=='Y';
            Release_based_on_Power_Law_initial(Counter)=0;
            Release_based_on_Power_Law_swollen(Counter)=0;
        end
        Release_based_on_first(Counter)=0;
        Release_based_on_second(Counter)=0;
    else
        N=length(x_zeros); % Number of bessel J terms
        Mass_t_Power_Law=zeros(1,N);
        Mass_t_Power_Law_Adjusted=zeros(1,N);
        if Ask=='Y';
            Mass_t_Power_Law_initial=zeros(1,N);
            Mass_t_Power_Law_swollen=zeros(1,N);
        end
        Mass_t_first=zeros(1,N);
        Mass_t_second=zeros(1,N);
        Summation_Power_Law=0;
        Summation_Power_Law_Adjusted=0;
        if Ask=='Y';
            Summation_Power_Law_initial=0;
            Summation_Power_Law_swollen=0;
        end
        Summation_first=0;
        Summation_second=0;
        if Ask=='Y' % Radius is not constant
            for M=1:N; % For varying radius
                Mass_t_Power_Law(M)=(4/(((a(n))^2)...
                 *((x_zeros(n,M))^2)))*...
                 exp((-Dij_Power_Law(n))*...
                 (x_zeros(n,M)^2)*Time(n));
                Mass_t_Power_Law_Adjusted(M)=(4/...
                 (((a(n))^2)*((x_zeros(n,M))^2)))...
```

```
                *exp((Dij_Power_Law_Adjusted(n))*...
                (x_zeros(n,M)^2)*Time(n));
            Mass_t_Power_Law_initial(M)=(4/...
                (((initial)^2)*((x_zeros_initial(M))...
                ^2)))*exp((-Dij_Power_Law_initial)*...
                (x_zeros_initial(M)^2)*Time(n));
            Mass_t_Power_Law_swollen(M)=(4/...
                (((swollen)^2)*((x_zeros_swollen(M))...
                ^2)))*exp((-Dij_Power_Law_swollen)*...
                (x_zeros_swollen(M)^2)*Time(n));
            Mass_t_first(M)=(4/(((a(n))^2)*...
                ((x_zeros(n,M))^2)))*exp((...
                -Dij_Power_Law)*(x_zeros(n,M)^2)*Time(n));
            Mass_t_second(M)=(4/(((a(n))^2)*...
                ((x_zeros(n,M))^2)))*exp((...
                -Dij_Power_Law_Adjusted)*...
                (x_zeros(n,M)^2)*Time(n));
            Summation_Power_Law=Summation_Power_Law+...
                Mass_t_Power_Law(M);
            Summation_Power_Law_Adjusted=...
                Summation_Power_Law_Adjusted+...
                Mass_t_Power_Law_Adjusted(M);
            Summation_Power_Law_initial=...
                Summation_Power_Law_initial+...
                Mass_t_Power_Law_initial(M);
            Summation_Power_Law_swollen=...
                Summation_Power_Law_swollen+...
                Mass_t_Power_Law_swollen(M);
            Summation_first=Summation_first+..
                Mass_t_first(M);
            Summation_second=Summation_second+...
                Mass_t_second(M);
        end
    else %Radius is constant
        for M=1:N; % For constant radius
            Mass_t_Power_Law(M)=(4/(((a)^2)*...
            ((x_zeros(M))^2)))*exp((-Dij_Power_Law)*...
            (x_zeros(M)^2)*Time(n));
            Mass_t_Power_Law_Adjusted(M)=(4/...
            (((a)^2)*((x_zeros(M))^2)))*exp((...
            -Dij_Power_Law_Adjusted)*...
            (x_zeros(M)^2)*Time(n));
            Mass_t_first(M)=(4/(((a)^2)*...
            ((x_zeros(M))^2)))*exp((-Dij_first)*...
            (x_zeros(M)^2)*Time(n));
            Mass_t_second(M)=(4/(((a)^2)*...
            ((x_zeros(M))^2)))*exp((-Dij_second)...
```

```
                    *(x_zeros(M)^2)*Time(n));
                    Summation_Power_Law=Summation_Power_Law+...
                     Mass_t_Power_Law(M);
                    Summation_Power_Law_Adjusted=...
                     Summation_Power_Law_Adjusted+...
                     Mass_t_Power_Law_Adjusted(M);
                    Summation_first=Summation_first+...
                     Mass_t_first(M);
                    Summation_second=Summation_second+...
                     Mass_t_second(M);
                end
            end
            Release_based_on_Power_Law(n)=1-...
              Summation_Power_Law;
            Release_based_on_Power_Law_Adjusted(n)=1-...
              Summation_Power_Law_Adjusted;
            if Ask=='Y';
                Release_based_on_Power_Law_initial(n)=1-...
                 Summation_Power_Law_initial;
                Release_based_on_Power_Law_swollen(n)=1-...
                 Summation_Power_Law_swollen;
            end
            Release_based_on_first(n)=1-Summation_first;
            Release_based_on_second(n)=1-Summation_second;
        end
    end
    %% Plot
    figure (1)
    plot(time,Release_Data,'.b','MarkerSize',20);
    hold on
    % Turn whatever data not required for plots into comments
    plot(Times,Power_Law,'k','LineWidth',5);
    plot(Time,Release_based_on_Power_Law,'g','LineWidth',5);
    plot(Time,Release_based_on_Power_Law_Adjusted,'r',...
         'LineWidth',5);
    plot(Time,Release_based_on_first,'c','LineWidth',5);
    plot(Time,Release_based_on_second,'m','LineWidth',5);
    if Ask=='Y';
        plot(Time,Release_based_on_Power_Law_initial,...
         'o c','LineWidth',5);
        plot(Time,Release_based_on_Power_Law_swollen,...
         '--m','LineWidth',5);
    end
    %plot(time,Expansion_Fit,'--k','LineWidth',5);
    set(gca,'FontSize',18);
    % Titles change based on what data is plotted
    % title('Release of NaCS from Gelatin Fibers');
```

```
% title('Release of NaCS from Gelatin Fibers with Fitted
% Power Law Equation');
% title('Release of NaCS from Gelatin Fibers with Mutual
% Diffusion Coefficient Solved from k Relation');
% title('Release of NaCS from Gelatin Fibers with Adjusted
% Mutual Diffusion Coefficient Solved from k Relation');
 title('Comparison of Release Models For NaCS in ...
     Gelatin Fibers With Different Solved Values for ...
     the Mutual Diffusion Coefficient')
% title('Release of NaCS from Gelatin Fibers with Mutual
% Diffusion Coefficient Solved from the First Three Terms
% of Expanded Diffusion Equation');
% title('Release of NaCS from Gelatin Fibers with Mutual
% Diffusion Coefficient Solved from Expanded Diffusion Eq.
% with Weighted Average')
xlabel('Time (Days)');
ylabel('Fractional Release Percent');
% Two legends are present since the legends change
% depending on what is plotted
legend('Measured Release Data','Power Law', ...
 'Release based on Dij from Power Law',...
 'Release based on adjusted Dij from Power Law', ...
 'Release based on Dij from expanded equation (first ...
 term)', 'Release based on Dij from expanded equation ...
 (second term)', 'Non-Linear Fit of Release Data',...
 'Location','SouthEast')
% legend('Measured Release Data', 'Release based on Dij
% from expanded equation (first)', 'Release based on Dij
% from expanded equation (second)', 'Non-Linear Fit of
% Release Data','Release based on Dij from Power Law Before
% Swell', 'Release based on Dij from Power Law After
% Swell','Location','SouthEast')
grid on
ylim([0,0.2])
hold off
```

APPENDIX B

MODIFCATIONS OF MATLAB CODING UTILIZED FOR CALCULATIONS TO STUDY OXYGEN RELEASE

Below are the sections that were modified in the code to adjust for oxygen release

Input of Oxygen Release (Section before Input of Release Data Manually Section)

```
%% Input Oxygen data
data= xlsread('chitosanmat1.xls');
count=length(data)*3;
data_point_count=length(data)*2+60;
time_length=data_point_count;
initial_oxygen_content=data(1,2);
Oxygen_release=zeros(data_point_count,1);
counter=1;
n=1;
N=1;
m=1;
timer=1;
Time_counter=1;
Oxygen_counter=1;
time=zeros(time_length,1);
while counter<=count;
     if counter<=181;
         Oxygen_release(Oxygen_counter)= data(n,2)...
         -initial_oxygen_content;
         time(Time_counter)=timer;
         timer=timer+1;
         Oxygen_counter=Oxygen_counter+1;
         Time_counter=Time_counter+1;
         n=n+1;
     elseif counter>181 && counter<=362;
         Oxygen_release(Oxygen_counter)=data(N,4)...
         -initial_oxygen_content;
         time(Time_counter)=timer;
         timer=timer+1;
         Oxygen_counter=Oxygen_counter+1;
         Time_counter=Time_counter+1;
         N=N+1;
     else counter>362;
         Oxygen_release(Oxygen_counter)=data(m,6)...
         -initial_oxygen_content;
         Check=Oxygen_release(Oxygen_counter);
         No_Value=isnan(Check);
         if No_Value==1;
         else
```

```
            Oxygen_counter=Oxygen_counter+1;
            time(Time_counter)=timer;
            Time_counter=Time_counter+1;
        end
        timer=timer+1;
        m=m+1;
    end
    counter=counter+1;
end

Total_Oxygen_Content=Oxygen_release(data_point_count,1);
Oxygen_Release=Oxygen_release;
```

Input Release Data Manually Section

```
Release_data=Oxygen_Release;
time=time;
last_data_point=length(Release_data);
Total_release=Release_data(last_data_point);
count=1;
Release_Data=Release_data;
while count<=last_data_point
    Release_Data(count)=Release_data(count)/Total_release;
    count=count+1;
end
```

Power Law Section

```
k=0.529; % k and n were found manually with the Matlab
% curve fitting app
n=0.2054;
c=-0.8552; % The c value is to account for the delay in
% measurement readings
Times=0:1:543;
Length=length(Times);
Power_Law=zeros(1,Length);
Counters=1; %Counter for Power Law Equation
while Counters<=Length
    Power_Law(Counters)=(k*Times(Counters)^n)+c;
    Counters=Counters+1;
end
```

Inputs in the Solve for Diffusion coefficient based on first term of expansion section

```
Ask='N';
d=(232.32*10^-9);
```

Inputs in the Making adjustments to Diffusion Coefficient to manually fit data section

```
adjustment_factor=.022;
```

Calculated Dij based on expansion fit

```
%% Calculated Dij based on expansion fit
A=0.03335;
B=-0.001404;
C=7.218*10^-9;
Expansion_Fit=zeros(time,1);
for n=1:data_point_count+1;
    Expansion_Fit(n)=A*(time(n))^(1/2)-B*time(n)-
     C*(time(n))^3/2;
end
time_expansion=time;
Dij_first=((A^2)*(a^2)*pi)/16;
Dij_second=(B)*(a^2);
Dij_third=((C^(2/3))*(a^2)*pi)/((pi/3)^(2/3));
```

Note: Titles were modified to reflect the proper titles.

APPENDIX C

MATLAB CODING FOR EFFECT OF RADIUS ON RELEASE

```
%% Power Law
k=0.05553; % k and n found from curve fitting app in Matlab
n=0.2466; % Curve fitting was done for the
time=0:1:42;
Length=length(time);
Power_Law=zeros(1,Length);
Counters=1; %Counter for Power Law Equation
while Counters<=Length
    Power_Law(Counters)=k*time(Counters)^n;
    Counters=Counters+1;
end
%% Defining Radius and Dij
initial=(580*10^-9)/2; % 10wt% IBO in Gelatin (458*10^-9)/2
% for 5wt%
swollen=(1.211*10^-6)/2; % 10wt% IBO in Gelatin
% (2.975*10^-6)/2 for 5wt%
last_data_point=length(time);
Radius_Increase=(swollen-initial)/(last_data_point-1);
a=initial:Radius_Increase:swollen;
Dij_Power_Law_initial=9e-16; %Keeping Dij constant
Dij_Power_Law_swollen=Dij_Power_Law_initial;
Dij_Power_Law=Dij_Power_Law_initial;

%% Enter the calculated Dij into diffusion equation
Time=time; % Time matrix for Dij plotting
Counter=length(time); % counter for the for statement
Release_based_on_Power_Law=zeros(Counter,1);
Release_based_on_Power_Law_initial=zeros(Counter,1);
Release_based_on_Power_Law_swollen=zeros(Counter,1);
x=0:0.001:500;
y=besselj(0,x);
count=length(x); % Upper Limit of bessel j search for zeros
x_zeros=zeros(1,159); % 159=> number of zeros for time
% length x
counter=1; % For bessel j function
Count=1; % Input for zeros

% Bessel J function
while counter<count;
    if y(counter)>0 && y(counter+1)<0;
        x_zeros(Count)=(x(counter)+x(counter+1))/2;
        Count=Count+1;
```

```
    elseif y(counter)<0 && y(counter+1)>0;
        x_zeros(Count)=(x(counter)+x(counter+1))/2;
        Count=Count+1;
    else
    end
    counter=counter+1;
end

% Adjusting Bessel J function to reflect Jo(a*alpha) where
% alpha is the roots
x_zeros_initial=x_zeros/initial;
x_zeros_swollen=x_zeros/swollen;
Number_Radius_Inputs=length(a);
X_Zeros=zeros(Number_Radius_Inputs,159);
Counts=1; % Counter for inputing Bessel J zeros when radius
% is not constant
while Counts<=Number_Radius_Inputs;
    for n=1:159;
        X_Zeros(Counts,n)=(x_zeros(1,n))/(a(Counts));
    end
    Counts=Counts+1;
end
x_zeros=X_Zeros;

% Calculating summation
for n=1:Counter; % Counter=number of time term
    if n==1;
        Release_based_on_Power_Law(Counter)=0;
        Release_based_on_Power_Law_initial(Counter)=0;
        Release_based_on_Power_Law_swollen(Counter)=0;
    else
        N=length(x_zeros); % Number of bessel J terms
        Mass_t_Power_Law=zeros(1,N);
        Mass_t_Power_Law_initial=zeros(1,N);
        Mass_t_Power_Law_swollen=zeros(1,N);
        Summation_Power_Law=0;
        Summation_Power_Law_initial=0;
        Summation_Power_Law_swollen=0;
        for M=1:N; % For varying radius
            Mass_t_Power_Law(M)=(4/(((a(n))^2)*...
            ((x_zeros(n,M))^2)))*...
            exp((-Dij_Power_Law)*...
            (x_zeros(n,M)^2)*Time(n));
            Mass_t_Power_Law_initial(M)=(4/...
            (((initial)^2)*((x_zeros_initial(M))^2)))...
            *exp((-Dij_Power_Law_initial)*...
            (x_zeros_initial(M)^2)*Time(n));
```

```
            Mass_t_Power_Law_swollen(M)=(4/...
            (((swollen)^2)*((x_zeros_swollen(M))^2)))*...
            exp((-Dij_Power_Law_swollen)*...
            (x_zeros_swollen(M)^2)*Time(n));
            Summation_Power_Law=Summation_Power_Law+...
            Mass_t_Power_Law(M);
            Summation_Power_Law_initial=...
            Summation_Power_Law_initial+...
            Mass_t_Power_Law_initial(M);
            Summation_Power_Law_swollen=...
            Summation_Power_Law_swollen+...
            Mass_t_Power_Law_swollen(M);
        end
        Release_based_on_Power_Law(n)=1-...
        Summation_Power_Law;
        Release_based_on_Power_Law_initial(n)=1-...
        Summation_Power_Law_initial;
        Release_based_on_Power_Law_swollen(n)=1-...
        Summation_Power_Law_swollen;
    end
end
%% Plot
figure (1)
plot(Time,Release_based_on_Power_Law,'g','LineWidth',5);
hold on
plot(Time,Release_based_on_Power_Law_initial,...
'--c','LineWidth',5);
plot(Time,Release_based_on_Power_Law_swollen,...
'--m','LineWidth',5);
set(gca,'FontSize',18);
title('Effect of Swelling on Release Profile From Fibers...
Represented by 10wt% IBO Crosslinked Gelatin Fibers')
xlabel('Time (Days)');
ylabel('Fractional Release Percent');
legend('Release based on a constant Dij and radius ...
swelling from initial to swollen radius', ...
'Release based on constant Dij and radius of fiber ...
staying at the initial radius','Release based on ...
constant Dij and radius of fiber staying at the ...
swollen radius','Location','SouthEast')
grid on
hold off
```

REFERENCES

1. Chew, S.Y., et al., *Sustained release of proteins from electrospun biodegradable fibers.* Biomacromolecules, 2005. **6**(4): p. 2017-2024.

2. Kim, M.S., et al., *Release kinetics and in vitro bioactivity of basic fibroblast growth factor: effect of the thickness of fibrous matrices.* Macromolecular Bioscience, 2011. **11**(1): p. 122-130.

3. Meinel, A.J., et al., *Electrospun matrices for localized drug delivery: current technologies and selected biomedical applications.* European Journal of Pharmaceutics and Biopharmaceutics, 2012. **81**(1): p. 1-13.

4. *Drug Delivery Systems: Methods in Molecular Biology*. K.K. Jain, Ed. 2008, Basel, Switzerland: Humana Press.

5. Crank, J., *The Mathematics of Diffusion*. 1975, New York, New York: Clarendon Press.

6. Dash, M., et al., *Chitosan - A versatile semi-synthetic polymer in biomedical applications.* Progress in Polymer Science, 2011. **36**(8): p. 981-1014.

7. Gomes, L. and E.R. Gomes, *Perfluorocarbons compounds used as oxygen carriers from liquid ventilation to blood substitutes.* Revista da Faculdade de Ciências da Saúde, 2007 **1**(4): p. 58-65.

8. Shen, X., M. Yang, and S.A. Tomellini, *Liquid chromatographic analysis of glucosamine in commercial dietary supplements using indirect fluorescence detection.* Journal of Chromatographic Science, 2007. **45**(2): p. 70-75.

9. Thakur, R.A., et al., *Electrospun nanofibrous polymeric scaffold with targeted drug release profiles for potential application as wound dressing.* International Journal of Pharmaceutics, 2008. **364**(1): p. 87-93.

10. *Controlled Release of Drugs: Polymers and Aggregate Systems*. 1989, New York, New York: VCH Publishers, Inc.

11. Kale, S.P. and S. Garg, *Prediction of the mutual diffusion coefficient for controlled drug delivery devices.* Computers & Chemical Engineering, 2012. **39**(0): p. 186-198.

12. Ritger, P.L. and N.A. Peppas, *A simple equation for description of solute release I. fickian and non-fickian release from non-swellable devices in the form of slabs, spheres, cylinders or discs.* Journal of Controlled Release, 1987. **5**(1): p. 23-36.

13. Goh, Y.-F., I. Shakir, and R. Hussain, *Electrospun fibers for tissue engineering, drug delivery, and wound dressing.* Journal of Materials Science, 2013. **48**(8): p. 3027-3054.

14. Ong, S.-Y., et al., *Development of a chitosan-based wound dressing with improved hemostatic and antimicrobial properties.* Biomaterials, 2008. **29**(32): p. 4323-4332.

15. Zamani, M., M.P. Prabhakaran, and S. Ramakrishna, *Advances in drug delivery via electrospun and electrosprayed nanomaterials.* International Journal of Nanomedicine, 2013. **8**(0): p. 2997-3017.

16. Riess, J.G. and M.P. Krafft, *Advanced fluorocarbon-based systems for oxygen and drug delivery, and diagnosis.* Artificial Cells, Blood Substitutes, and Immobilization Biotechnology, 1997. **25**(1-2): p. 43-52.

17. National Institute of Standards and Technology. *Perfluorotributylamine*. [Web] 2011 2011 [cited 2014 March 23, 2014]; Available from: http://webbook.nist.gov/cgi/cbook.cgi?ID=C311897&Mask=200.

18. Goh, F., et al., *Limited beneficial effects of perfluorocarbon emulsions on encapsulated cells in culture: experimental and modeling studies.* Journal of Biotechnology, 2010. **150**(2): p. 232-239.

19. Ko, J.H., et al., *Characterization of cross-linked gelatin nanofibers through electrospinning.* Macromolecular Research, 2010. **18**(2): p. 137-143.

20. Young, S., et al., *Gelatin as a delivery vehicle for the controlled release of bioactive molecules.* Journal of Controlled Release, 2005. **109**(1-3): p. 256-274.

21. Sigma Aldrich. *D-Glucosamine 6-sulfate* [Web] 2014 [cited 2014 March 23, 2014]; Available from: http://www.sigmaaldrich.com/catalog/product/sigma/g8641?lang=en&region=US.

22. Flangea, C., et al., *Discrimination of GalNAc (4S/6S) sulfation sites in chondroitin sulfate disaccharides by chip-based nanoelectrospray multistage mass spectrometry.* Central European Journal of Chemistry, 2009. **7**(4): p. 752-759.

23. Zeeman, R., *Cross-linking of Collagen-Based Materials*. Enschede, Netherlands: Febodruk BV. 1991. Ph.D Dissertation, University of Twente.

24. Skoog, D.A.H.F.J.C.S.R., *Principles of Instrumental Analysis*. 2007, Belmont, California: Brooks/Cole : Thomson Learning.

25. *Vernier Optical DO Probe*. [Web] 2014 [cited 2014 April 15, 2014]; Available from: http://www.vernier.com/products/sensors/dissolved-oxygen-probes/odo-bta/.

26. Le, D.T., *Smart Bandage: A Novel Hemostatic And Oxygen Releasing Biomaterial*, in *Biomedical Engineering*. 2014, M.S. Thesis, New Jersey Institute of Technology.

27. Enobakhare, B.O., D.L. Bader, and D.A. Lee, *Quantification of sulfated glycosaminoglycans in chondrocyte/alginate cultures, by use of 1,9-dimethylmethylene blue.* Analytical Biochemistry, 1996. **243**(1): p. 189-191.

28. Stone, J.E., et al., *Interaction of 1,9-dimethylmethylene blue with glycosaminoglycans.* Ann Clin Biochem, 1994. **31**(2): p. 147-52.

29. Saul, J.M. and D.F. Williams, *Principles of Regenerative Medicine*. 2011, New York, New York: Academic Press.